2000

Mon. Not. R. Astron. Soc. **000**, 000–000 (2000)

Radio-quiet quasar environments at $0.5 \leq z \leq 0.8$

Margrethe Wold,[1§] Mark Lacy,[2] Per B. Lilje[3] and Stephen Serjeant[4]
[1] *Stockholm Observatory, SE-133 36 Saltsjöbaden, Sweden*
[2] *IGPP, Lawrence Livermore National Laboratory, 7000 East Avenue, Livermore, CA 94550, USA, and Department of Physics, University of California, 1 Shields Avenue, Davis, CA 95616, USA*
[3] *Institute of Theoretical Astrophysics, University of Oslo, P.O. Box 1029 Blindern, N-0315 Oslo, Norway*
[4] *Astrophysics Group, Imperial College London, Blackett Laboratory, Prince Consort Road, London SW7 2BZ, U.K.*

Accepted 0000. Received 0000; in original form 0000

ABSTRACT
We have quantified the galaxy environments around a sample of $0.5 \leq z \leq 0.8$ radio-quiet quasars using the amplitude of the spatial galaxy–quasar correlation function, $B_{\rm gq}$. The quasars exist in a wide variety of environments, some sources are located in clusters as rich as Abell class 1–2 clusters, whereas others exist in environments comparable to the field. We find that on average, the quasars prefer poorer clusters of $\approx$ Abell class 0, which suggests that quasars are biased tracers of mass compared to galaxies. The mean $B_{\rm gq}$ for the sample is found to be indistinguishable from the mean amplitude for a sample of radio-loud quasars matched in redshift and optical luminosity. These observations are consistent with recent studies of the hosts of radio-quiet quasars at low to intermediate redshifts, and suggest that the mechanism for the production of powerful radio jets in radio-loud quasars is controlled by processes deep within the active galactic nucleus itself, and is unrelated to the nature of the hosts or their environments.

Key words: galaxies: clustering – galaxies: active – galaxies: clusters – quasars: general

1 INTRODUCTION

The study and interpretation of the differences and similarities between radio-loud and radio-quiet quasars (RLQs and RQQs, hereafter) has kept astronomers busy for a long time. The spectral energy distributions of RLQs and RQQs differ only in points of detail at all wavelength bands, apart from the radio. Both quasar types possess broad emission lines and have a stellar appearance in even the highest resolution optical images. They also show the same evolution in number density with a peak at $z \sim 2$–3, but the RQQs outnumber the RLQs by a factor of 10. RQQs have radio luminosities 2–3 orders of magnitude lower than their radio-loud counterparts, and on radio maps they are compact with typically only a weak, flat-spectrum component coincident with the optical nucleus. On the other hand, the RLQs have extended lobes of radio emission with hotspots at the outer edges of the radio structure. The radio-emitting lobes are fed by powerful jets emerging from a bright, central core, but RQQs can also have jet-like structures (Blundell et al. 1996; Blundell & Beasley 1998), although with bulk kinetic powers $\sim 10^3$ times lower than for RLQs (Miller, Rawlings & Saunders 1993). This suggests that both quasar populations have jet-producing central engines, but that the efficiency of the jet production mechanism is very different in the two cases.

One way to learn more about how the two quasar types relate, is to study their host galaxies and their galactic environment. A longstanding belief that RQQs are hosted by spiral galaxies and RLQs by ellipticals is now being questioned. Recent studies (e.g. Dunlop et al. 1993; McLeod & Rieke 1994; Taylor et al. 1996; Bahcall et al. 1997; Boyce et al. 1998; McLure et al. 1999; Hughes et al. 2000) have found that powerful quasars at $z0.5$, both radio-loud and radio-quiet, seem to exist in galaxies with luminosities $> L^*$, the luminosity at the break in the luminosity function. Still, a clear picture has not emerged, with some studies claiming a high fraction of disk morphologies amongst the radio-quiets (e.g. Percival et al. 2000), whilst others suggest that nearly all quasars are in giant ellipticals (e.g. McLure et al. 2000). Besides the technical difficulties associated with studying host galaxies, quasar optical luminosity and selection effects may affect the results. E.g. the perhaps somewhat artificial distinction between Seyfert galaxies and quasars at $M_V = -23$ leads to confusion as to whether an active galactic nucleus (AGN) is a quasar or a Seyfert. Seyfert galaxies are spirals, are found at lower redshifts and have lower AGN luminosities than RLQs, so very few RLQs exist for compar-

§Email: wold@astro.su.se

ison. Selection effects may therefore have caused spirals to be preferred as hosts of RQQs and giant ellipticals to be preferred as hosts of RLQs.

Quasar environments have also been investigated on much larger scales than those of typical host galaxies. RLQs at $0.5z0.8$ are often found to be associated with groups or clusters of galaxies (Yee & Green 1987; Ellingson, Yee & Green 1991a; Wold et al. 2000 (hereafter Paper I)), with richnesses varying from poor groups to Abell Class 1 clusters or richer. This is perhaps not surprising since giant elliptical galaxies, found to be the hosts of powerful RLQs, frequently reside in the centres of galaxy clusters. But what is the galaxy environment like for RQQs in this redshift range, and how does it compare with the environment around RLQs with comparable AGN luminosities?

In this paper, we try to answer this question by investigating a sample of RQQs matched in redshift and optical luminosity to a sample of RLQs analysed in Paper I. We quantify the galaxy environment using the amplitude of the spatial galaxy–quasar cross-correlation function, $B_{\rm gq}$, often referred to as the 'clustering amplitude'. The first attempt at comparing the environments around RLQs and RQQs using the clustering amplitude was made by Yee & Green (1984), who found only a marginal difference. Later, Yee & Green (1987) did deeper imaging of the same RQQ fields, and added more RLQ fields to the sample. They repeated the analysis with improved parameters, and obtained an even smaller difference, but due to the small number of RQQs (seven) in their sample, they were unable to draw any firm conclusions.

The problem was later addressed by Ellingson et al. (1991a), who also used the clustering amplitude to quantify the Mpc-scale environment around a sample of 65 $17.5 < m < 19$ quasars at $0.3 < z < 0.6$, of which half were radio-quiet. They found that the RLQs exist more often in rich galaxy environments than the RQQs do, which was believed to support the RQQ/spiral host–RLQ/elliptical host hypothesis. Since this study, there has been little work aimed at comparing the environments of the two quasar populations at moderate redshifts, but at both lower and higher redshifts several studies indicate that contrary to the conclusion reached by Ellingson et al., the galaxy environment around RLQs and RQQs is similar. But also here, a clear picture has not yet emerged, since several other studies seem to support Ellingson et al's conclusion.

Some investigators use the clustering amplitude, which makes comparison between studies similar to ours easier, whereas other studies have other aims, and therefore use different techniques and methods. These studies can basically be divided into two categories. The first category includes measurements of the *angular* galaxy–quasar cross-correlation function by cross-correlating quasar catalogues with galaxy counts. The aim is to establish whether optically and X-ray selected quasars (i.e. mostly RQQs) can be used as unbiased tracers of galaxies. This is important to know, since the large quasars surveys currently in progress, like the 2dF (Shanks et al. 2000) and the Sloan Digital Sky Survey (Fan et al. 1999), will be used to study large-scale structure out to high redshifts, but require knowledge about how quasars are biased with respect to galaxies. The second category includes more or less qualitative searches for galaxies in quasar and radio galaxy fields at both high and low redshifts. E.g. data obtained for host galaxy studies, at typically $z0.3$, can be utilized for environment studies, but the high resolution imaging required to study hosts often results in a small field of view and therefore a relatively small sampling radius.

Investigations of the galaxy–quasar angular correlation function are often concerned with scales larger than typical cluster scales. At low redshifts, Smith, Boyle & Maddox (1995) selected 169 ($z < 0.3$) optically identified quasars from the EMSS (Einstein Medium Sensitivity Survey), and cross-correlated their positions with $B_J < 20.5$ galaxies from the APM galaxy catalogues in a region of radius 05 centered on the quasar. They found that the amplitude of the angular galaxy–quasar cross-correlation function was identical to that of the APM galaxy angular correlation function, implying that the quasars inhabit regions of space similar to that of normal galaxies. (At $z = 0.3$, 05 corresponds to almost 10 Mpc). In a follow-up study, Smith, Boyle & Maddox (2000) cross-correlated X-ray selected quasars at $0.3 \leq z \leq 0.7$ with $V \leq 23$ galaxies on CCD images. They found a 2σ excess around the $z \leq 0.5$ quasars on scales < 1 arcmin, but no excess for the $z > 0.5$ quasars. As an overall result, they claimed that the galaxy–quasar correlation function is consistent with that for faint galaxies. The quasars in their sample span a wide range in luminosity, from $M_V \approx -27$ to -20 ($H_0 = 50\ {\rm km\,s^{-1}\,Mpc^{-1}}$), but no difference between high and low luminosity sub-samples was observed.

Croom & Shanks (1999) cross-correlated 150 quasars selected both in the optical and in X-rays with $b_J < 23$ galaxies on AAT (Anglo-Australian Telescope) photographic plates. They found the angular cross-correlation to be marginally negative, indicative of a small anti-correlation, possibly due to gravitational lensing. Most of the quasars in their sample lie at redshifts 1.0–2.2, and they claimed to reach M^* at $z \approx 1$ and $M^* - 1$ at $z \approx 1.5$. Possibly, this is not deep enough, as even M^* might be too shallow into the luminosity function to detect excess galaxies at $z = 1.0$–2.2 (Yee & López-Cruz 1999).

Searches for galaxies in quasar and radio galaxy fields in connection with host studies have been conducted by e.g. Smith & Heckman (1990) who generated catalogues of companion galaxies within $100h^{-1}$ Mpc of 31 $z < 0.3$ quasars and 35 powerful radio galaxies. They found that RQQs only have half the number of nearby, bright companions as RLQs and radio galaxies at the 95 per cent confidence level. Somewhat inconsistent with Smith & Heckman's result is the result obtained by Fisher et al. (1996) who found no significant difference in the environments around optically luminous RLQs (six) and RQQs (14) at $z0.3$. Supporting Fisher et al's result is the recent study by McLure & Dunlop (2000), who quantified the environments around 44 powerful, $z \approx 0.2$ AGN, of which 13 were RLQs and 21 were RQQs (their sample includes Fisher et al's quasars). They found the mean clustering amplitude for the two quasar samples to be consistent with each other, and corresponding to Abell richness class 0 clusters. Dunlop et al. (1993), studying quasar hosts in the near-infrared, also discuss companion galaxies. Their sample consisted of 14 RLQs and 14 RQQs at $z < 0.35$ matched in redshift and V magnitude. They found that the surface density of bright ($K > 18$) companion galaxies was a factor of ≈ 2.5 higher than in the field, and the excess was similar for both RLQs and RQQs.

The high redshift studies of quasar environments typically concentrate at $z1$. Quasars (and radio galaxies) are used as pointers to high redshift galaxies in order to learn about galaxy formation and evolution and to search for high redshift (proto)clusters. Galaxies, and even clusters, are certainly found at $z1$ using this method (e.g. Dickinson 1994; Deltorn et al. 1997; Hall & Green 1998; Tanaka et al. 2000, Chapman, McCarthy & Persson 2000; Best 2000).

Hintzen, Romanishin & Valdes (1991) and Boyle & Couch (1993) investigated $0.9 < z < 1.5$ RLQs and RQQs, respectively. Hintzen et al. found a significant galaxy excess within a 15 arcsec radius ($\approx$ 160 kpc) centered on the quasars in their sample, whereas Boyle & Couch (1993) found no evidence for excess. However, Boyle & Couch's RQQs are 20 times fainter in the optical than the RLQs studied by Hintzen et al., and Boyle & Couch discuss this as a possible cause for the discrepancy.

In contrast to this, Hutchings, Crampton & Johnson (1995) found on average a $> 5\sigma$ excess of galaxies around both RLQs and RQQs (14 in total) at $z \approx 1.1$. They saw no significant difference between RLQ and RQQ environments, which was found to consist of compact groups of starbursting galaxies. Also, Hutchings (1995a), who looked at galaxy companions to seven $z = 2.3$ quasars (only one RLQ) in the R-band found an overall $> 5\sigma$ excess in a ~ 1 arcmin region around the quasars. However, Hutchings et al. (1999), using near-infrared imaging of both RLQs and RQQs at $0.9 < z < 4.2$, note that the RQQs occupy poorer environments than the RLQs, but do not draw any firm conclusions due to the small and still incomplete sample. Teplitz, McLean & Malkan (1999) also report that the number counts of galaxies in RQQ fields at $0.95 < z < 1.5$ in J- and K'-band is comparable to the field counts, but their data is not very deep (only reaching $\approx M^*$ at $z \approx 1$).

In summary, although the results seem to differ, the consensus about hosts and environments of RQQs – that they are typically late-type galaxies in poor environments – is being increasingly questioned. Several recent observations at high and low redshifts seem to indicate that RQQs live in richer than average galaxy environment, and powerful RQQs at $z0.5$ are found in luminous, possibly early-type, galaxies.

Apart from Ellingson et al's (1991a) study at $0.3 < z < 0.6$, there have been no attempts to investigate what environments RQQs prefer at intermediate redshifts. We have therefore obtained data on a sample of 20 RQQs at $0.5 \leq z \leq 0.8$, and quantified the galaxy richness in the quasar fields using a similar analysis as Ellingson et al. The sample is described in Section 2, where we also discuss the radio loudness of some of the quasars. In Section 3, we describe the observations and our observing strategy. The control fields used in the analysis are also commented upon here, especially how the galaxy counts vary with galactic latitude. The analysis using the clustering amplitude is briefly overviewed in Section 4, before the results are presented in Section 5. In Section 5.1 we examine the colours and the radial distribution of the galaxies in the quasar fields. Using the clustering amplitude allows us to compare our results with some of the above mentioned studies, and this is done in Section 6, and in Section 7 we are able to directly and consistently compare with the sample of RLQs that was presented in Paper I. Finally, we discuss the results in Section 8, and draw the conclusions in Section 9.

Our assumed cosmology has $H_0 = 50\ \mathrm{km\,s^{-1}\,Mpc^{-1}}$, $\Omega_0 = 1$ and $\Lambda = 0$.

2 THE SAMPLE

The RQQs were selected from three optical surveys with different flux limits in order to cover a wide range in AGN luminosity (B-band) within the given redshift range. Eight of the quasars are from the faint ($B21$) Durham/AAT UVX survey of Boyle et al. (1990) (designated 'BFSP') and ten are from the intermediate luminosity ($16 b_J 18.9$) Large Bright Quasar Survey (LBQS) by Hewett, Foltz & Chaffee (1995). There are also two high-luminosity quasars in the sample, selected from the $B16.6$ Bright Quasar Survey (BQS) by Schmidt & Green (1983). The sample is listed in Table 1 along with information about the observations.

The BQS and the Durham/AAT UVX survey are based on the UV-excess selection technique which finds $z < 2.2$ quasars with stellar-like appearance and excess emission in the UV. The LBQS is an objective prism survey, from which quasar candidates are essentially selected by their blue colour. The LBQS and the Durham/AAT UVX survey are complete, but the BQS survey has been found to be incomplete by a factor of 3.4 (Goldschmidt et al. 1992), possibly due to photometry errors. Also, the BQS is known to have an anomalously high radio-loud fraction at bright optical magnitudes, $M_B < -24$, compared to other optically selected samples (LaFranca et al. 1994), and Hooper et al. (1996) find that the radio-loud fraction at faint optical luminosities is lower in the BQS than in the LBQS. We have checked that inclusion of the two BQS quasars does not affect our results.

The RLQ sample that we compare with in Section 7 consists of 21 steep-spectrum RLQs at $0.5 \leq z \leq 0.8$ covering the wide radio luminosity range $23.8 \leq \log\left(L_{408\mathrm{MHz}}/\mathrm{W\,Hz^{-1}\,sr^{-1}}\right) \leq 26.7$. This sample was drawn from two different radio/optical flux-limited samples, the Molonglo/APM Quasar Survey (Serjeant 1996; Maddox et al., in preparation; Serjeant et al., in preparation) and the 7C Quasar survey (Riley et al. 1999). For details about the RLQ sample, we refer to Paper I.

In order to check if some of the RQQs were detected at radio wavelengths, we extracted image cutouts at the quasar positions from the 1.4 GHz NVSS* (Condon et al. 1998) and the VLA FIRST† survey (Becker, White & Helfand 1995) and examined them in AIPS. We found seven quasars that were detected in either both or just one of the surveys and list the radio fluxes of these in Table 2. For the other quasars, we set a 3σ detection as upper limit since the 1σ noise level for the NVSS and FIRST are 0.5 and 0.17 $\mathrm{mJy\,beam^{-1}}$, respectively.

The quasars with radio detections are the two BQS quasars, three of the LBQS quasars and two of the faint BFSP quasars, and we have marked these with 'R' in Table 2. One of these quasars, BQS 1538+447, looks resolved on the FIRST map and appears to have FRI morphology.

Can these seven (out of 20) radio-detected quasars be

* NRAO/VLA Sky Survey

† Faint Images of the Radio Sky at Twenty-centimeters

Table 1. The quasar sample and log of observations. All images were obtained using the HiRAC equipped with a 1k SiTe CCD with pixel scale 0.176 arcsec, unless otherwise is specified in footnotes. In the 6th column, we list the FWHM of the seeing in the combined image (in the longest wavelength filter when there are observations in two filters).

Quasar	z	Filter	Exp. time (s)	Date	Seeing (arcsec)	Remarks
LBQS 0007−0003	0.698	I	4×600	96/07/23	1.1	photometric
LBQS 0020−0300	0.580	V, R	4×600	96/07/25	0.8	dust
BFSP 12344−0021*	0.753	I	5×300	98/04/28	0.7	variable transparency
		I	6×300‡	00/01/03		photometric
BFSP 12355+0107†	0.720	I	9×300	97/05/14	0.5	photometric
BFSP 12364−0053*	0.727	I	8×300	99/05/19,23	0.9	variable transparency
		I	1×300‡	00/01/03		photometric
BQS 1333+176*	0.554	R	4×600	00/01/03	0.7	photometric
BFSP 15152+0244†	0.608	R	4×600	97/05/14	0.6	photometric
BFSP 15196+0220	0.742	I	4×600	96/07/24	0.8	dust
BFSP 15199+0247	0.768	R, I	5×600	96/07/23	0.6	photometric
BFSP 15202+0236	0.765	R, I	4×600	96/07/22	0.6	photometric
BQS 1538+477	0.770	R, I	4×600	96/07/21	0.6	photometric
BFSP 22011−1857	0.615	V, R	4×600	96/07/21	1.0	photometric
LBQS 2235+0054	0.529	V, R	4×600	96/07/21	1.0	photometric
LBQS 2238+0133	0.714	R, I	4×600	96/07/22	0.7	photometric
LBQS 2239−0055	0.680	R, I	4×600	96/07/23	0.9	photometric
LBQS 2245−0055	0.801	R, I	5×600	96/07/24	1.3	dust
LBQS 2348+0210	0.504	V, R	4×600	96/07/24	1.3	dust
LBQS 2348+0148	0.749	I	4×600	96/07/25	0.8	dust
LBQS 2350−0012	0.561	V, R	4×600	96/07/23	0.9	photometric
LBQS 2353−0153	0.672	R, I	4×600	96/07/22	0.6	photometric

*Imaged using ALFOSC with a 2k Loral CCD with pixel scale 0.189 arcsec.

†Imaged with the HiRAC camera, but with a 2k Loral CCD with pixel scale 0.11 arcsec.

‡Exposures taken during photometric conditions in order to calibrate the other images obtained under less photometric conditions.

classified as RQQs? The distinction between RLQs and RQQs is not clear-cut, and different definitions exist. Indeed it seems likely that there is a continuum in radio-loudness, with RLQs representing the extreme of the distribution in radio luminosity at a given absolute magnitude (White et al. 2000). Nevertheless, a distinction is often made based on radio luminosity and/or the ratio of radio to optical flux density, R. According to the radio luminosity criterion, a quasar is radio-loud if $P_{5\rm GHz} > 10^{24}$ W Hz^{-1} sr^{-1}, or $P_{5\rm GHz} > 1.3 \times 10^{25}$ W Hz^{-1}, whereas according to the criterion used by e.g. Kellermann et al. (1989), a quasar is radio-loud if $R10$. A much used definition of R is the ratio of the rest frame flux at 5 GHz to the B-band flux, and here we choose Sramek & Weedman's (1980) definition, $R = S_{5\rm GHz}/S_{2500}$, which uses the flux density at rest frame 5 GHz and 2500 Å (corresponding to B-band when $z \sim 0.7$). The usefulness of the R-parameter is not clear, e.g. Goldschmidt et al. (1999) argue that R is physically meaningful only if the radio and optical luminosity is linearly correlated, and that there are various reasons that this might not be the case (Goldschmidt et al. and references therein).

To calculate the R-parameter, we assumed that both radio and optical flux density scales as $S_\nu \propto \nu^{-\alpha}$, and computed rest frame flux densities at 5 GHz and 2500 Å. The rest frame flux density at 5 GHz was found according to

$$S_{5\rm GHz} = S_{1.4\rm GHz} \left(\frac{5}{1.4}\right)^{-\alpha} (1+z)^{\alpha-1},$$

where we used the NVSS flux as $S_{1.4\rm GHz}$ when available, since this is most sensitive to extended structures. The radio power was also calculated,

$$P_{5\rm GHz} = 4\pi d_{\rm L}^2 \, S_{5\rm GHz},$$

where d_L is the luminosity distance to the quasar. The optical flux density at rest frame 2500 Å was found from the m_B magnitudes of the quasars (determined from the images, see details in Section 3) using the relation

$$S_{2500} = S_B \left(\frac{4400}{2500}\right)^{-\alpha} (1+z)^{\alpha-1},$$

where $\log S_B = -22.35 - 0.4 m_B$ (Longair 1981). In Table 2, we list the rest frame radio and optical flux densities, the $R_{5\rm GHz}$ parameter and the radio power.

In the above calculations, we assumed a spectral index of $\alpha = 0.5$ for both the radio and the optical spectra, but for four of the quasars we estimated radio spectral indices by extrapolating between the NVSS/FIRST flux densities and flux densities measured at 5 GHz by Kellermann et al.

Table 2. Radio fluxes at 1.4 GHz from NVSS and FIRST image cutouts. Quasars with radio detections in NVSS or FIRST (or both) are marked with an R in the first column. For the other quasars, we give upper limits that correspond to 3σ detections. Rest frame fluxes at 5 GHz and 2500 Å are denoted $S_{5\rm GHz}$ and S_{2500}, and their ratio is $R_{5\rm GHz}$. The radio power is denoted $P_{5\rm GHz}$, and α_r is the radio spectral index between 1.4 and 5 GHz.

Quasar	NVSS (mJy)	FIRST (mJy)	$S_{5\rm GHz}$ (mJy)	α_r	S_{2500} (mJy)	$R_{5\rm GHz}$	$P_{5\rm GHz}$ W Hz^{-1}
LBQS 0007−0003	< 1.5	< 0.5	<0.61	0.50	0.10	< 6.1	$< 1.6\times10^{24}$
LBQS 0020−0300	< 1.8	no map	<0.76	0.50	0.21	< 3.6	$< 1.4\times10^{24}$
BFSP 12344−0021$^{\rm R}$	4.8	5.2	1.92	0.50	0.03	64.0	6.1×10^{24}
BFSP 12355+0107	confused	< 0.5	<0.20	0.50	0.02	< 10.0	$< 5.8\times10^{23}$
BFSP 12364−0053	< 1.5	< 0.5	<0.60	0.50	0.01	< 60.0	$< 1.8\times10^{24}$
BQS 1333+176$^{\rm R}$	37.6	no map	18.54	0.32*	0.60	30.9	3.0×10^{25}
BFSP 15152+0244	< 1.5	< 0.5	<0.63	0.50	0.02	< 31.5	$< 1.3\times10^{24}$
BFSP 15196+0220	< 1.5	< 0.5	<0.60	0.50	0.03	< 20.0	$< 1.9\times10^{24}$
BFSP 15199+0247	< 1.5	< 0.5	<0.60	0.50	0.03	< 20.0	$< 2.0\times10^{24}$
BFSP 15202+0236$^{\rm R}$	< 1.5	1.0	0.40	0.50	0.01	40.0	1.3×10^{24}
BQS 1538+447$^{\rm R}$	95.2	85.4	26.28	1.02*	1.00	26.3	8.8×10^{25}
BFSP 22011−1857	< 1.5	no map	<0.62	0.50	0.05	< 12.4	$< 1.3\times10^{24}$
LBQS 2235+0054$^{\rm R}$	< 1.5	0.83	0.94	$-0.65^\dagger$	0.02	47.0	1.4×10^{24}
LBQS 2238+0133	< 1.5	no map	<0.61	0.50	0.22	< 2.8	$< 1.7\times10^{24}$
LBQS 2239−0055	< 1.5	< 0.5	<0.61	0.50	0.12	< 5.1	$< 1.6\times10^{24}$
LBQS 2245−0055$^{\rm R}$	< 1.5	1.3	0.51	0.50	0.30	1.7	1.9×10^{24}
LBQS 2348+0210$^{\rm R}$	41.8	no map	25.05	0.12†	0.17	143.4	3.3×10^{25}
LBQS 2348+0148	< 1.5	no map	<0.60	0.50	0.08	< 7.5	$< 1.9\times10^{24}$
LBQS 2350−0012	< 1.5	< 0.5	<0.64	0.50	0.32	< 2.0	$< 1.1\times10^{24}$
LBQS 2353−0153	< 1.5	< 0.5	<0.61	0.50	0.57	< 1.1	$< 1.5\times10^{24}$

*Spectral index found between flux at 1.4 GHz and flux measured at 5 GHz by Kellermann et al. (1989)

†Spectral index between 1.4 GHz flux and flux measured at 8.4 GHz by Hooper et al. (1996)

(1989) or at 8.4 GHz by Hooper et al. (1996), denoted $\alpha_{\rm r}$ in Table 2. We found that BQS 1538+477 has a steep radio spectrum with $\alpha^5_{1.4} = 1.02$, but the spectrum flattens at high frequency, with $\alpha^{10}_{8.7} = -0.19$ (Falcke, Sherwood & Patnaik 1996), so it is therefore likely that the bright core is flat spectrum and possibly variable, but the extended emission is steep-spectrum. The spectrum of LBQS 2235+0054 is somewhat unusual with $\alpha^{8.4}_{1.4} = -0.65$, i.e. the flux density rises with increasing frequency. This could be due to synchrotron self-absorption at low frequencies or perhaps thermal absorption.

As seen in Table 2, six of the seven radio-detected quasars have $R > 10$, and classify as radio-loud according to Kellermann et al's (1989) criterion, but only three of these, the two BQS quasars and LBQS 2348+0210, have radio luminosities greater than 1.3×10^{25} W Hz^{-1} and qualify both criteria.

Miller et al. (1993), in a study of BQS quasars, found a group of quasars with radio luminosities at 4.8 GHz in the range $\sim$ 1.3–4.0 $\times\ 10^{24}$ W Hz^{-1} ($H_0 = 50$ km s^{-1} Mpc^{-1}, $q_0 = 0$) that did not tightly follow the emission line–radio luminosity correlation, and termed these 'radio-intermediate quasars'. It was suggested that they could be Doppler-boosted RQQs with Lorentz factors of ~ 5. In terms of the R-parameter, it is common to classify quasars with $1 < R_{5\rm GHz} < 100$ as radio-intermediate and quasars with $R_{5\rm GHz} \leq 1$ as radio-quiet. According to this, all but one of the seven radio-detected quasars are radio-intermediate, the exception being LBQS 2348+0210 with $R_{5\rm GHz} = 143.4$.

Falcke et al. (1996) find that the division line at $R = 10$ between RLQs and RQQs leads to inconsistencies with the Unified Scheme, since they find a high fraction of flat-spectrum, core-dominated quasars in the BQS. According to orientation-based Unified Schemes these are relativistically beamed radio sources with extended lobe emission, and should therefore be rare and have radio flux densities higher than the steep-spectrum sources. Falcke et al. term these radio-intermediate quasars, and also suggest that they are relativistically boosted radio-weak quasars. They propose to use both the R-parameter *and* the spectral index to divide between RLQs and RQQs, and that the division line between radio-loud and radio-quiet is set at $R = 250$ for flat-spectrum sources and at $R = 25$ for steep-spectrum sources, so that the radio-intermediate quasars have R-parameters in the range 25–250.

Blundell & Beasley (1998) also point out that if the criterion for radio-loudness is based on the extended radio emission in quasars, the radio-intermediate quasars would classify as radio-quiet. This would however not be the case for BQS 1538+447, since its extended radio flux is 53.9 mJy (total NVSS flux minus peak FIRST flux), corresponding to 5.0×10^{25} W Hz^{-1} at 5 GHz.

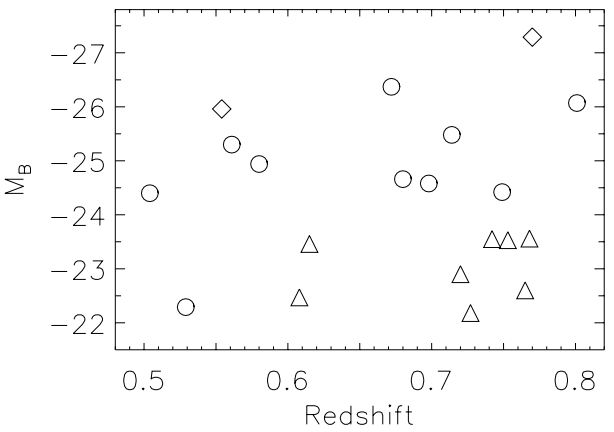

Figure 1. Absolute B magnitudes of the quasars as a function of redshift. Diamonds: bright BQS quasars, circles: intermediate-luminosity LBQS quasars, triangles: faint BFSP quasars.

The seven quasars discussed above clearly have radio powers much lower than typical RLQs ($\sim 10^{26}$–10^{27} W Hz^{-1}), and if not radio-quiet, may classify as either radio-intermediate or radio-weak. However, we have checked that our results are not affected by the presence/absence of these quasars.

3 OBSERVATIONS AND DATA REDUCTION

Most of the data were obtained using the High Resolution Adaptive Camera (HiRAC) at the 2.56-m Nordic Optical Telescope (NOT) during 1996 July 21–25. The HiRAC was equipped with a 1k SiTe CCD with a pixel scale of 0.176 arcsec, giving a field of view of 3×3 arcmin. Two quasar fields were imaged in May 1997, also using the HiRAC, but with a Loral 2k chip with pixel scale 0.11 arcsec, giving a 3.7×3.7 arcmin field of view. Images of three more quasar fields were obtained during observing runs at the NOT in 1998, 1999 and 2000 using the ALFOSC (Andalucia Faint Object Spectrograph and Camera) in imaging mode, equipped with a 2k Loral CCD with pixel scale 0.189 arcsec, and a field of view of 6.5×6.5 arcmin. The bulk of the data were obtained under photometric conditions, and the seeing FWHM is less than one arcsec in 15 out of 20 fields.

Since we are attempting to detect galaxies that are physically associated with the quasars, the filters were chosen to give preference to early-type galaxies with strong 4000 Å breaks at the quasar redshifts. The spectral energy distribution of early-type galaxies is characterized by a strong break at 4000 Å with most of the energy emitted at wavelengths longer than 4000 Å. For an early-type galaxy at $z \geq 0.67$ the 4000 Å break moves from R into I-band, so for the $z \geq 0.67$ quasars we used I-band imaging and for the $z < 0.67$ quasars we chose R-band. Twelve of the fields were also imaged in two filters, either V and R, or R and I, depending on the redshift of the quasar so as to straddle the 4000 Å break.

Typically, the integrations were divided into four exposures of 600 s each, offsetting the telescope 10 arcsec between each exposure to avoid bad pixels and cosmetic defects from falling consistently on the same spots. The I-band images from 1997–2000 (three fields) have a prominent fringing pattern due to interference of night sky lines. We therefore took 9–11×300 s exposures of these fields in order to obtain a sufficient number of images to construct a fringe frame. The fringe frame was made by taking the median of nine I-band images taken close in time, and used to flatten the background with by dividing out the fringes. Apart from this flat fielding technique to remove fringes, the data were reduced as described in Paper I using standard IRAF reduction tasks.

We also observed standard star fields during each night in order to calibrate magnitudes to the standard Johnson photometric system. During the 1996 and 1997 runs, we observed fields by Christian et al. (1985), and for the other observing runs we selected standard stars by Landolt (1992).

The two fields from 1998 and 1999 (BFSP 12344−0021 and BFSP 12364−0053) were imaged as back-up targets during another programme that required photometric and sub-arcsec seeing conditions, so the transparency is somewhat reduced in these frames. We therefore took exposures of the same fields under photometric conditions in January 2000 to enable a proper photometric calibration.

For photometry and object detection we processed the images in FOCAS (Faint Object Classification and Analysis System, e.g. Valdes (1989)), as described in Paper I. Each detected object was classified by using a template PSF (a 15×15 array) formed from 4-6 selected stars in each image, and a record of FOCAS total magnitudes and positions of the detections were made by excluding objects classified as 'multiple', 'long' or 'noise'. The detections were examined by eye and objects coinciding with spikes of bright stars were removed from the records.

As described in Paper I, we performed completeness simulations in the images, and these simulations show that the data are complete down to 24.0 in V, 23.5 in R and 23.0 in I, with errors of ±0.3 mag at the limits.

The quasar fields lie at high galactic latitudes $46^\circ < |b| < 76^\circ$ and the galactic reddening is $E\,(B-V) < 0.063$ in all fields. We corrected for galactic extinction using an electronic version of the maps by Burstein & Heiles (1982) and the Galactic extinction law by Cardelli, Clayton & Mathis (1989).

Unless the quasar was saturated in the image, we determined its apparent magnitude in either R or I, and thereafter converted to B assuming an optical power-law spectrum, $S_\nu \propto \nu^{-\alpha}$, with $\alpha = 0.5$ and zero points in B, R and I as given by Longair (1981). The B magnitudes were thereafter converted to absolute magnitudes by assuming a K-correction equal to $2.5\,(\alpha-1)\log(1+z)$.

Three of the quasars were saturated in the images (BQS 1333+176, BQS 1538+477 and LBQS 2348+0210) so we used apparent B and B_J magnitudes as given in the catalogues, except for BQS 1333+176 for which Yee, Green & Stockman (1986) have determined an r magnitude. The B_J magnitude for LBQS 2348+0210 was converted to B by assuming $B = B_J + 0.09$ (Metcalfe et al. 1991), and the Gunn r magnitude of BQS 1333+176 was first converted to R by assuming $r = R + 0.43 + 0.15\,(B-V)$ (Kent 1985) and a $B-V$ colour of 0.3 (i.e. $B-V$ of a quasar with optical spectral index $\alpha = 0.5$), and thereafter to B as described above.

Fig. 1 shows the distribution of the quasars in the z–M_B plane, and the M_B magnitudes are also listed in Table 4.

3.1 Control fields

Since we are concerned with investigating if there is an excess of galaxies in the quasar fields, we aim to have a good determination of the background counts. For this purpose, we obtained images of random fields in the sky at approximately the same galactic latitudes as targets in our AGN sample. The control fields were described in Paper I, so here it suffices to mention that these fields were imaged as part of our AGN environment survey, and therefore have the same depth and were obtained in exactly the same manner as the quasar fields. This is important in order to get a robust estimate of the galaxy richness in the quasar fields (Yee & López-Cruz 1999).

In Paper I, we averaged the counts in the control fields in order to obtain a good determination of the background counts, and we also found that the slopes of the background galaxy number counts agreed well with that found by other investigators, e.g. Smail et al. (1995). Due to the clustered nature of field galaxies, the errors in the galaxy counts are expected to be $\approx 1.3\sqrt{N}$ (Yee & López-Cruz 1999). However, the variation in the counts from control field to control field is larger than this, presumably due to the small areas surveyed in each field (typically 3×3 arcmin), but also due to a variation in the counts with galactic latitude, especially in the I-band control fields.

This can be seen in Fig. 2 where we have plotted the number of galaxies brighter than the completeness limits from raw counts in the control fields as a function of galactic latitude, with $1.3\sqrt{N}$ error bars. The counts in the quasar fields within a 0.5 Mpc radius centered on the quasar are also plotted, and we have included the RLQ fields from Paper I. The error bars on the counts in the quasar fields are intentionally left out for clarity. It is seen that six of the eight I-band control fields lie at galactic latitudes between 45–60°, where also the bulk of the quasar fields are found. The remaining two lie at $|b| \approx 30°$, and were obtained in order to get a handle on the counts here since two fields in our radio galaxy sample (to be published in a future paper) lie at lower latitudes.

The counts in the two $|b| \approx 30°$ fields have a mean of 16.94±2.3 arcmin^{-2}, whereas the fields between 45 and 60° have a mean of 11.53±1.6 arcmin^{-2}, so the background counts appear to increase towards lower latitudes. Presumably this is due to faint, red stars as the background counts in R do not seem to vary as much with latitude. It is seen that the bulk of the quasar and control fields lie at latitudes between 40 and 60°. Nevertheless, in addition to using the average background counts, as we did in Paper I, we also here make a correction for the variation in the counts with latitude.

In I-band, a least square fit to the eight data points weighted with the error bars gives a relation for the background counts of $N(I) = -0.32|b| + 26.6$. This is shown by the solid line in Fig. 2, and we call this Model 1. A straight line through the mean values of the two low latitude and the six high latitude fields gives a less steep relation of $N(I) = -0.25|b| + 24.5$, as shown by the dotted line. This relation is named Model 2.

As mentioned above, the R-band background counts show a weaker dependence on galactic latitude. The corresponding Model 1 for the R counts is $N(R) = -0.15|b| + 18.6$, and by drawing a line through the mean of the seven fields at 40–60° and the mean of the two $|b| \approx 30°$ fields, we get that Model 2 for the R-band counts is $N(R) = -0.17|b| + 19.4$ galaxies per arcmin^2. Outside the ranges of the sloped lines in Fig. 2, we have used the constant values corresponding to the endpoints of the relations.

We have chosen to let the background counts follow these relations when correcting for background galaxies in the quasar fields, but we have also used the average of all control fields, named Model 3. Details about these models can be found in Table 3. We have also included the V-band control fields in this table since these were used to find the excess in five quasar fields that were also imaged in R. Since there are only two V-band control fields (at $|b| = 574$ and 467), we have used as Model 1, a relation that has the same slope as the R counts, but is normalized to the mean V-band counts.

4 ANALYSIS

To quantify the excess counts in the quasar fields we have used the amplitude, $B_{\rm gq}$, of the spatial galaxy–quasar cross-correlation function, $\xi(r) = B_{\rm gq} r^{-\gamma}$, where $\gamma = 1.77$. The amplitude is evaluated at a fixed radius of 0.5 Mpc at the quasar redshift, corresponding to ≈ 1 arcmin at $z = 0.7$ and has units of Mpc$^{1.77}$. Longair & Seldner (1979) showed how it can be used to estimate the clustering about any point in the Universe using galaxy counts, and it has subsequently been widely used to quantify galaxy environment around different types of AGN (e.g. Yee & Green 1987; Yates, Miller & Peacock 1989; Ellingson et al. 1991a; Smith, O'Dea & Baum 1995; Wurtz et al. 1997; DeRobertis, Yee & Hayhoe 1998; McLure & Dunlop 2000). In Paper I we used it to quantify the environments around RLQs, and here we apply the same analysis to the RQQs. We therefore refer to Paper I for a more detailed description of the analysis, and give only a brief summary here (see also Longair & Seldner 1979; Yee & Green 1987).

First, the amplitude, $A_{\rm gq}$, of the *angular* cross-correlation function is found. This is easily obtainable from the data since it is directly proportional to the number of excess galaxies within the 0.5 Mpc radius centered on the quasar. Thereafter, $B_{\rm gq}$ is obtained from the following expression

$$B_{\rm gq} = \frac{\mathcal{N}_{\rm g} A_{\rm gq}}{\Phi(m_{\rm lim}, z)\, I_\gamma} d_\theta^{\gamma-3},$$

where $\mathcal{N}_{\rm g}$ is the average surface density of background galaxies, d_θ is the angular diameter distance to the quasar and $I_\gamma = 3.78$ is an integration constant.

In the denominator, $\Phi(m_{\rm lim}, z)$ is the luminosity function integrated down to the completeness limit of the data, thus giving the number of galaxies per unit volume at the quasar redshift seen in the flux-limited data. We have used a Schechter function to evaluate the integral, with characteristic magnitude $M^*_{AB}(B) = -20.83$ and slope

Table 3. Various relations used for the galaxy background counts. In Model 1 and 2 the counts are dependent on the absolute value of the galactic latitude $|b|$, whereas Model 3 is just the average counts. The error in the average given in the last column is the standard deviation in the mean, and the other errors were calculated as $1.3\sqrt{N}$.

	Model 1		Model 2		Model 3
Filter	Range (°)	N (arcmin^{-2})	Range (°)	N (arcmin^{-2})	N (arcmin^{-2})
I	$30.0 \leq \|b\| \leq 57.1$	$-0.32\|b\|+26.6$	$30.1 \leq \|b\| \leq 51.6$	$-0.25\|b\|+24.5$	12.36±4.38
I	$\|b\| < 30.0$	17.07±5.37	$\|b\| < 30.1$	16.94±5.35	12.36±4.38
I	$\|b\| > 57.1$	8.50±3.79	$\|b\| > 51.6$	11.53±4.41	12.36±4.38
R	$29.2 \leq \|b\| \leq 57.2$	$-0.15\|b\|+18.6$	$29.7 \leq \|b\| \leq 48.5$	$-0.17\|b\|+19.4$	12.51±2.69
R	$\|b\| < 29.2$	14.07±4.88	$\|b\| < 29.7$	14.45±4.94	12.51±2.69
R	$\|b\| > 57.2$	9.74±4.06	$\|b\| > 48.5$	11.30±4.37	12.51±2.69
V	$30.0 \leq \|b\| \leq 57.4$	$-0.15\|b\|+18.23$			10.19±6.88
V	$\|b\| < 30.0$	13.60±4.79			10.19±6.88
V	$\|b\| > 57.4$	9.40±4.0			10.19±6.88

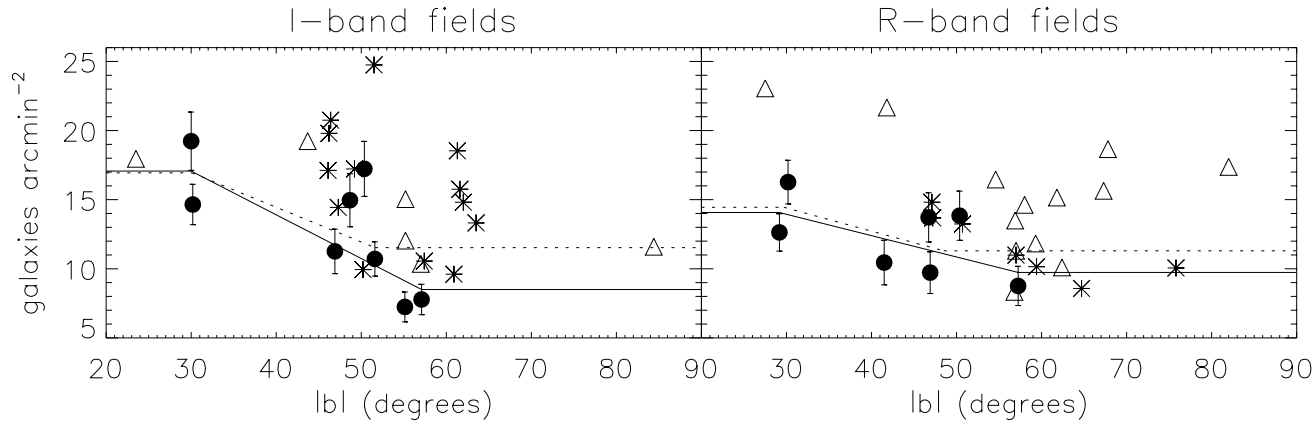

Figure 2. The filled circles show the counts of galaxies in the I- and R-band control fields as a function of galactic latitude (absolute value). The number of galaxies in the quasar fields are also plotted using asterisks for the RQQs and triangles for the RLQs. The solid and dotted lines show the relations for the background counts as a function of galactic latitude, corresponding to Model 1 and Model 2, respectively (see text and Table 3 for details).

$\alpha = -0.89$ based on Lilly et al's (1995) estimation of the CFRS (Canada-France Redshift Survey) luminosity function in the $0.5 \leq z \leq 0.75$ redshift interval. Since the integrated Schechter function is proportional to the characteristic density, ϕ^*, the $B_{\rm gq}$ estimator becomes inversely proportional to it, and therefore very sensitive to its value. Yee & Green (1987) and Yee & López-Cruz (1999) have advocated the importance of choosing ϕ^* in such a way that it is consistent with the data. In Paper I, we explain how we used the CFRS luminosity function to construct galaxy counts that were fitted to the observed counts in the control fields. The fitting gave $\phi^*_V = 0.0065$, $\phi^*_R = 0.0072$ and $\phi^*_I = 0.0052$ Mpc^{-3}, and we use these numbers in our computation of $\Phi\,(m_{\rm lim}, z)$.

Yee & López-Cruz (1999) have examined the robustness of $B_{\rm gc}$ (index 'gc' means galaxy–cluster centre) on a sample of 47 low-z Abell clusters, and find that it is a robust estimator of galaxy richness in clusters. They apply a number of tests, and find that $B_{\rm gc}$ is fairly robust provided the normalization of the luminosity function reproduces the observed galaxy counts. Under this condition, varying e.g. M^* causes variations in $B_{\rm gc}$ of ≈ 10 per cent. Also counting down to different absolute magnitude limits produces systematic variations of only a few per cent, but the best and most reliable results are obtained if one counts down to 1–2 magnitudes fainter than M^*. In the I-band images we have reached approximately 1.7 mag past M^*, and in the R-band data, about 2 mag (see last column of Table 4).

5 GALAXY EXCESS IN QUASAR FIELDS

We counted the number of galaxies within the 0.5 Mpc radius in the quasar fields and averaged the counts for the R and I-band data, i.e. for the seven $z < 0.67$ and the 13 $z \geq 0.67$ quasar fields. The average counts are shown in Fig. 3, where we also have plotted the average galaxy counts in the control images. The error bars of the background galaxy count were calculated as $1.3\sqrt{N}$. There is a clear excess of faint galaxies at $I > 20$, but the galaxy

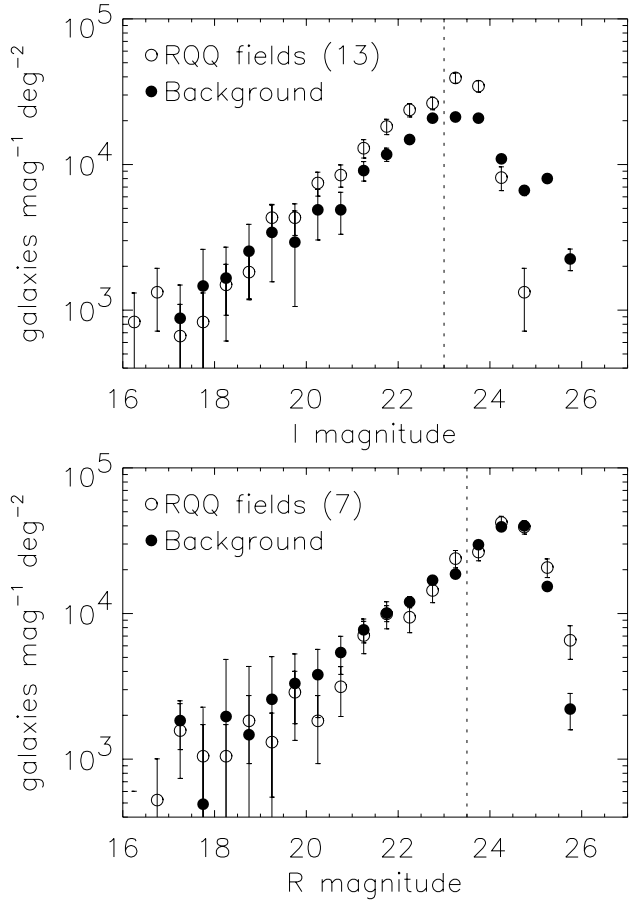

Figure 3. The open circles show the average galaxy counts within the 0.5 Mpc circle in the quasar fields, and the filled circles show the counts in the control fields. The vertical dotted lines mark the completeness limits, $I = 23.0$ and $R = 23.5$.

counts in the R-band fields show no average excess above the background.

For each quasar field, the net excess of galaxies within the 0.5 Mpc radius, $N_{\rm net}$, was calculated by subtracting the background counts according to Model 1–Model 3 from the counts in the quasar fields. Thereafter, the amplitudes $A_{\rm gq}$ and $B_{\rm gq}$ were obtained. The results are shown in Table 4, where we, for each model of the background counts, show the net excess, $N_{\rm net}$, the significance, σ, of the excess, and the clustering amplitude, $B_{\rm gq}$.

Since the background counts were scaled to the area of the 0.5 Mpc circle, $N_{\rm net}$ is not an integer. The significance, σ, was calculated as $N_{\rm net}/1.3\sqrt{N_{\rm b}}$, and the uncertainty in $B_{\rm gq}$ as

$$\frac{\Delta B_{\rm gq}}{B_{\rm gq}} = \frac{\left(N_{\rm net} + 1.3^2 N_{\rm b}\right)^{1/2}}{N_{\rm net}}.$$

(Yee & López-Cruz 1999).

In the last column of Table 4, we show approximately how many magnitudes fainter than M^* an Sa galaxy with apparent magnitude $m = m_{\rm lim}$ is. This demonstrates that we are close to the recommended $M^* + 2$ in all the fields so that a reliable estimate of $B_{\rm gq}$ is obtained. By transforming $M^*_{AB}\,(B) = -20.83$ to R and I, assuming $B_{AB} = B - 0.17$ (Oke 1972) and using colours of a zero redshift Sa galaxy model, $B - V = 0.74$, $V - R = 0.68$ and $R - I = 0.57$ (Guiderdoni & Rocca-Volmerange 1988), we found that $M^*_R = -22.08$ and $M^*_I = -22.65$.

The mean clustering amplitude using Model 1 for the background counts is 336±77 Mpc$^{1.77}$, whereas using Model 2 and Model 3 gives lower mean amplitudes of 212±74 and 210±82 Mpc$^{1.77}$. The correction in the background counts to account for galactic latitude is therefore more drastic in Model 1, giving a higher mean $B_{\rm gq}$, but the three mean values are nevertheless within the errors of each other. (The errors we give for the mean $B_{\rm gq}$'s are standard deviations in the mean.) Also, for each field, the three $B_{\rm gq}$'s given in Table 4 are consistent with each other, and their variation should give some indication of the real errors that are involved in this analysis.

The mean clustering amplitude in the quasar fields, regardless of which model is used for the background counts, is higher than the local galaxy–galaxy correlation amplitude of ≈ 60–70 Mpc$^{1.77}$ (Davis & Peebles 1983; Loveday et al. 1995; Guzzo et al. 1997), so on average, we find that the RQQs are not located in field-like environments, but rather seem to prefer groups or poorer clusters.

Using a χ^2 test, we compared the distribution of the significances of the excess to that of a normal distribution (which is what we expect if there are no excess galaxies around the quasars), and find a probability of 9×10^{-20} (Model 1) that the distribution is equal to that of a normal distribution. For Model 2 and 3, we get probabilities of 9×10^{-9} and 1×10^{-10}. Excluding the seven radio-detected quasars, we get probabilities (for Model 1 to 3) of 1.0×10^{-10}, 1.1×10^{-3} and 4.4×10^{-5} that the distribution of σ's is equal to a normal distribution. Furthermore, excluding the two BQS quasars, the probabilities become 5×10^{-10}, 5×10^{-4} and 7×10^{-6}. These very low probabilities agree with the visual impression from Fig. 8, where the $B_{\rm gq}$'s of both RLQs and RQQs are plotted as a function of redshift and M_B. The low probabilities are a strong result, and can imply either an average density enhancement or a variance in the environments greater than expected, and most likely, both are present in the data.

This adds more weight to the result that RQQs are on average not located in field-like environments. However, the environmental richness varies between individual fields; some fields have no significant excess, whereas other appear to be very rich in galaxies. There are five fields with a $> 2\sigma$ excess irrespective of how the background is calculated. The richest field among these is the field around BQS 1538+447 with a clustering amplitude in the range 1100–1200 Mpc$^{1.77}$ and a galaxy excess of ≈ 40–50. In Paper I we argued that an amplitude of ≈ 740 Mpc$^{1.77}$ corresponds roughly to Abell richness class 1, so the cluster candidate around BQS 1538+447 may even qualify as an Abell class 2 cluster. Four other fields have galaxy excesses of 20–30 galaxies and amplitudes 500 Mpc$^{1.77}$ and are probable Abell class 1 clusters. BFSP 15199+0247 and 15202+0236 have amplitudes in the range 700–800 Mpc$^{1.77}$, whereas LBQS 2239−0055 and 2353−0153 have somewhat smaller amplitudes of 400–500 Mpc$^{1.77}$.

As Fig. 3 shows, the R-band fields have a galaxy surface density close to that in the control fields, and the mean clustering amplitude for these, 71±34 Mpc$^{1.77}$, is consistent with

Table 4. The results of the analysis of galaxy counts in the RQQ fields. For each of the three models for the background counts (see Table 3), the net excess, $N_{\rm net}$, the significance of the excess, σ, and the clustering amplitude, $B_{\rm gq}$, are listed. The absolute B magnitude of the quasar is M_B, and ΔM in the last column shows how many magnitudes into the luminosity function the completeness limit extends, i.e. $M^* + \Delta M$. All numbers are based on galaxy counts in either R or I depending on whether the quasar redshift is < 0.67 or ≥ 0.67.

		Model 1			Model 2			Model 3			ΔM
Quasar	M_B	$N_{\rm net}$	σ	$B_{\rm gq}$	$N_{\rm net}$	σ	$B_{\rm gq}$	$N_{\rm net}$	σ	$B_{\rm gq}$	
LBQS 0007−0003	−24.58	3.9	0.6	84±155	−6.4	−0.8	−137±165	−6.9	−0.8	−146±166	1.9
LBQS 0020−0300	−24.94	−4.4	−0.6	−68±119	−10.4	−1.2	−161±123	−14.8	−1.7	−230±126	1.9
BFSP 12344−0021	−23.53	21.0	3.1	529±208	11.1	1.4	278±218	10.7	1.3	268±219	1.7
BFSP 12355+0107	−22.90	16.4	2.4	371±182	6.2	0.8	140±192	5.8	0.7	131±192	1.8
BFSP 12364−0053	−22.18	24.5	3.5	565±197	14.3	1.8	331±206	13.9	1.7	321±206	1.8
BQS 1333+176	−25.96⋆	1.4	0.2	20±116	−4.8	−0.6	−68±119	−9.4	−1.0	−133±122	2.1
BFSP 15152+0244	−22.47	8.3	1.0	144±156	8.7	1.0	151±156	4.8	0.5	83±158	1.8
BFSP 15196+0220	−23.55	17.6	2.2	428±222	13.9	1.6	337±226	18.3	2.3	443±222	1.7
BFSP 15199+0247	−23.56	29.6	3.7	777±255	25.8	3.1	678±259	29.9	3.7	785±255	1.6
BFSP 15202+0236	−22.60	26.4	3.3	689±250	22.7	2.7	592±253	26.9	3.4	703±250	1.6
BQS 1538+477	−27.29†	48.0	6.4	1276±271	43.1	5.4	1147±275	43.0	5.4	1144±275	1.6
BFSP 22011−1857	−23.46	8.5	1.0	152±157	7.3	0.9	131±158	3.1	0.4	55±161	1.7
LBQS 2235+0054	−22.29	13.6	1.5	176±125	14.1	1.6	182±125	9.8	1.1	127±127	2.2
LBQS 2238+0133	−25.48	10.3	1.3	229±194	6.2	0.7	138±197	9.6	1.2	215±194	1.8
LBQS 2239−0055	−24.66	22.3	2.8	450±187	17.6	2.1	356±191	19.5	2.4	394±190	2.0
LBQS 2245−0055	−26.07	−1.8	−0.2	−52±219	−6.3	−1.5	−185±225	−5.4	−0.7	−158±224	1.5
LBQS 2348+0210	−24.40††	4.2	0.5	50±105	−1.2	−0.1	−14±107	−6.1	−0.7	−73±109	2.4
LBQS 2348+0148	−24.42	6.9	1.0	172±183	−3.1	−0.4	−76±194	−3.5	−0.4	−86±194	1.7
LBQS 2350−0012	−25.30	1.7	0.2	25±118	−4.4	−0.5	−64±122	−9.0	−1.0	−130±124	2.0
LBQS 2353−0153	−26.37	35.3	5.0	699±183	24.7	3.0	489±191	24.2	2.9	480±191	2.0

⋆Found from Gunn r magnitude as observed by Yee et al. (1986)
†Computed from B found by Schmidt & Green (1983)
††Computed from B_J given by Hewett et al. (1995)

that of galaxies in the local universe (23±50 and −43±50 Mpc$^{1.77}$ for Model 2 and 3). For the 13 I-band fields the mean clustering amplitude is 478±96 Mpc$^{1.77}$ (314±101 and 346±106 Mpc$^{1.77}$ for Model 2 and 3, respectively). It might therefore seem that there is an apparent trend with redshift since the R-band fields represent the $z < 0.67$ quasars, but the current sample of 20 objects is too small and span a too narrow redshift range to test this properly.

In principle, we are interested in the full distribution function for the clustering amplitude, e.g. when the data are compared with models. The distribution will be positively skewed with a long tail to the right since we do not observe fields with negative $B_{\rm gq}$'s comparable in absolute value to the most positive $B_{\rm gq}$ values. For a positively skewed distribution, the median will always be smaller than the mean, and for our sample the median $B_{\rm gq}$ is 131 Mpc$^{1.77}$ (Model 3). A model for formation of RQQs should be able to reproduce both the mean amplitude and the intrinsic scatter in $B_{\rm gq}$. Thus the intrinsic scatter is equally important as the mean amplitude. The scatter (standard deviation) of the $B_{\rm gq}$ distribution is $\sigma_{B_{\rm gq}} = 365 \pm 58$ Mpc$^{1.77}$ (Model 3), and this includes both intrinsic scatter and measuring uncertainty. We have used a measuring uncertainty of $\Delta B_{\rm gq} \approx 185 \pm 48$ Mpc$^{1.77}$, and estimated the intrinsic scatter, $\sigma_{\rm int}$, assuming that $\sigma^2_{\rm int} = \sigma^2_{B_{\rm gq}} + \Delta B^2_{\rm gq}$, giving $\sigma_{\rm int} = 315 \pm 73$ Mpc$^{1.77}$. As expected, the intrinsic scatter is large, but difficult to estimate due to the large measuring uncertainty in $B_{\rm gq}$. In Table 7 we list values of $\sigma_{\rm int}$, mean and median $B_{\rm gq}$'s that we get by using the different models for the background galaxy counts.

Since 12 of the fields were imaged in two filters, we also computed $B_{\rm gq}$ in the fields taken in the shortest wavelength filter, and list the results in Table 5. The mean amplitudes are 220±92 and 120±93 Mpc$^{1.77}$ for Model 1 and Model 3, respectively (Model 2 gives values intermediate between these two). For comparison, the mean amplitudes for the same 12 fields obtained in the reddest filters are 367±120 and 276±125 Mpc$^{1.77}$. So, the mean amplitudes are lower, but still within the errors of each other, and on average, the excess is detected in both filters. There are two fields which have significantly higher $B_{\rm gq}$ in I than in R, and these are BQS 1538+447 and LBQS 2353−0153, with $B_{\rm gq}$ approximately a factor of two higher in I than in R, suggestive of a fair amount of red galaxies in these fields. This is what we expect if there are many red, early-type galaxies with strong 4000 Å breaks at the quasar redshift.

Although the overall trend is that $B_{\rm gq}$ is larger in the reddest filters, there are 3–4 fields where the opposite is seen. This can, apart from in one case, probably be attributed to measurement errors since these are fields with no significant excess. The exception is BFSP 22011−1857, with a $\sim 2\sigma$ excess in V, but with no excess in R. The clustering amplitude deduced from the R image lies in the range 50–150, whereas it is ≈ 470 Mpc$^{1.77}$ in V-band. This field was care-

Table 5. The results of the analysis of the quasar fields that were imaged in two filters, here in the shortest wavelength filter, i.e. in V for the $z < 0.67$ quasars and in R for the $z \geq 0.67$ quasars. The completeness limit in V is 24.0.

		Model 1			Model 3		
Quasar	Filter	$N_{\rm net}$	σ	$B_{\rm gq}$	$N_{\rm net}$	σ	$B_{\rm gq}$
LBQS 0020−0300	V	−13.0	−1.7	−341±181	−16.1	−2.0	−420±185
BFSP 15199+0247	R	22.0	2.7	594±251	19.3	2.3	521±254
BFSP 15202+0236	R	16.9	2.1	449±240	14.3	1.7	380±243
BQS 1538+477	R	27.3	3.7	745±246	18.4	2.2	503±255
BFSP 22011−1857	V	14.6	1.8	464±283	15.4	1.9	490±282
LBQS 2235+0054	V	10.0	1.2	201±187	13.2	1.6	265±184
LBQS 2238+0133	R	1.2	0.1	25±175	−2.1	−0.3	−44±178
LBQS 2239−0055	R	17.2	2.3	322±162	7.7	0.9	144±169
LBQS 2245−0055	R	−0.2	−0.0	−7±229	−8.9	−1.1	−283±242
LBQS 2348+0210	V	8.8	1.1	157±157	5.6	0.7	99±159
LBQS 2350−0012	V	−7.9	−1.0	−187±175	−11.0	−1.3	−261±178
LBQS 2353−0153	R	11.9	1.6	218±152	2.4	0.3	44±159

fully checked in order to verify that there are more galaxies in the V image than in the R image. There are two possible explanations for this, one is that there is a foreground concentration of bluer galaxies toward this quasar, the other is that it might be a cluster with a blue galaxy population at the quasar redshift.

5.1 Properties of the excess galaxies

Elliptical and early-type spiral galaxies in clusters are known to form a tight sequence in the color-magnitude diagram, the so-called 'red sequence'. It is the strongly evolved 4000 Å breaks in these galaxies that make their colour red, since metals in the cool atmospheres of giant stars absorb much of the radiation blueward of 4000 Å.

In the conventional models, elliptical galaxies are believed to form during a monolithic collapse at $z > 2$ and evolve passively after an initial starburst (e.g. Larson 1975; Arimoto & Yoshii 1987). An alternative model that has received much attention lately is the hierarchical formation scenario, where elliptical galaxies are formed by mergers of disk systems (Toomre & Toomre 1972). It has been shown that this scenario is also consistent with the presence of the red sequence in galaxy clusters (Kauffmann & Charlot 1998).

Here, we have picked the four richest quasar fields that were imaged in two filters, and examined the colours of the galaxies. The four fields are BFSP 15199+0247, BFSP 15202+0236, BQS 1538+447 and LBQS 2353−0153, with $B_{\rm gq}500$ Mpc$^{1.77}$ and a 3σ excess. The mean redshift for these quasars is $\langle z \rangle = 0.74 \pm 0.02$. Fig. 4 shows a colour-magnitude diagram of galaxies in these fields, where we have excluded stars at $I < 21$ (as explained later in this section).

There is a hint of a red sequence at $R - I \approx 1.5$–1.7 in this figure, i.e. tentative evidence that these fields likely contain galaxy clusters at $z \approx 0.7$–0.8. Very few galaxy clusters are know at $z0.7$, but judging from other work, the red sequence is expected to occur at $1.3R - I2.0$. (Luppino & Kaiser 1997; Clowe et al. 1998, Lubin et al. 2000). Also spectral synthesis models predict that this is the colour expected for early-type galaxies at redshifts 0.7–0.8 (e.g. Fukugita, Shimasaku & Ichikawa 1995).

The red sequence is known to steepen toward brighter magnitudes, and this can possibly also be seen in Fig. 4. The steepening toward brighter magnitudes is believed to be caused by the mass-metallicity relation in the galaxies, the most luminous and massive galaxies having a higher metal content and therefore also stronger 4000 Å breaks. The slope of the red sequence in clusters is also expected to flatten toward higher redshifts. As the formation epoch of a galaxy is approached, the stellar populations in the massive ellipticals become younger and bluer relative to the low-mass systems, and by measuring the slope of the red sequence as a function of redshift, one can constrain the formation epoch of the galaxies. Gladders et al. (1998) have studied clusters in the redshift range $0 < z < 0.75$, and find that there is little evidence for a change in the slope prior to $z = 0.75$, thereby concluding that the formation epoch occurs at $z > 2$. For two clusters at $z = 0.756$, Gladders et al. find a slope of -0.0566 ± 0.0066, and a least square fit to the galaxies at $19 \leq I \leq 21.5$ and $1.3 < R - I < 2.0$ in Fig. 4 gives a slope of $\approx -0.07 \pm 0.03$, consistent with Gladders et al.

Ferreras & Silk (2000) also show that the red sequence in clusters can by used to discriminate between the two formation scenarios, monolithic vs hierarchical, particularly at the bright end. The two formation scenarios predict significantly different bright-end slopes at high redshifts, and a number of $z > 0.7$–0.8 clusters must be observed to test this. Since few clusters are known at these redshifts, AGN-selected clusters are therefore useful targets for such studies.

Can the tentative red sequence at $R - I \approx 1.5$–1.7 be caused by stars? This is probably not the case, since we do not expect many stars in these high latitude fields (these four quasar fields lie at latitudes 46–61°). Nevertheless, the I-band counts in the control fields seem to indicate that red stars are present in the fields at some level. To investigate this further, we made an attempt to identify stars in these images by their half-light radii, as shown in Fig. 5.

This was done using the IMCAT software by N. Kaiser, developed to measure the distortion of faint galaxies induced by gravitational potentials of galaxy clusters. The software

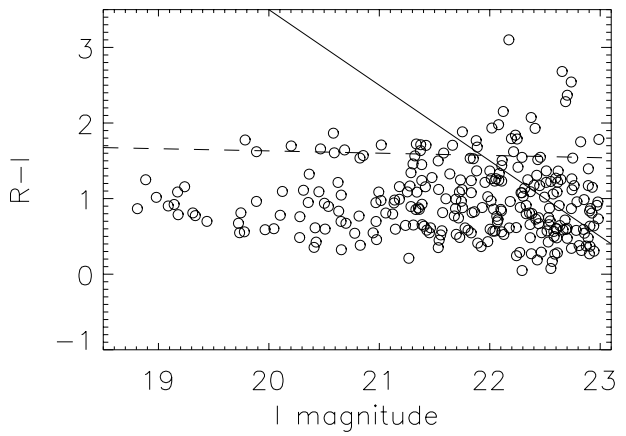

Figure 4. Colour-magnitude diagram of galaxies in the four richest quasar fields, showing a hint of a red sequence at $R-I \approx 1.5$–1.7. Possible stars at $I < 21$ are excluded. The dashed line shows a least square fit to the galaxies at $19 < I \leq 21.5$ and $1.3 < R-I < 2.0$ with a slope of -0.07 ± 0.03. The solid line marks the completeness limit in R.

automatically measures the half-light radii of galaxies in the images, a feature that is not included in FOCAS. However, IMCAT uses a different detection algorithm than FOCAS. In FOCAS, objects are detected by locating connected regions above a certain threshold, whereas IMCAT smooths the images with gaussian filters using a range of different radii (see Kaiser, Squires & Broadhurst (1995) for details).

In the upper plot in Fig. 5, the stellar locus is seen along a half-light radius of ≈ 0.4 arcsec, corresponding to a seeing FWHM of ≈ 0.8 arcsec, and stars can clearly be separated from galaxies down to $I \approx 21$. We selected objects with half-light radii between the two horizontal, solid lines (corresponding to half-light radii of 1.9 and 2.5 pix, or 0.33 and 0.44 arcsec) and plotted them in a colour-magnitude diagram as shown in the lower plot. The colour-magnitude distribution of stars is expected to be bimodal, with disk stars at the blue end and spheroid stars at the red end (Bahcall & Soneira 1981). The bimodal distribution is not clearly seen here, presumably due to the small number of stars, but there seems to be a gap at $0.8 < R-I < 1.3$. Bahcall & Soneira find that the stars in the Galactic spheroid have typical colours of $R-I \approx 1.6$–2.2, and that the bluer disk population has $R-I \approx 0.1$–0.8, which appears to agree roughly with what we see here.

At $19 < I \leq 23$ and at colours $1.3 < R-I < 2.0$, where we suspect the red sequence to be, 18 out of 90 objects have half-light radii corresponding to the stellar locus in Fig. 5, i.e. four–five stars per field, so the red sequence cannot be caused exclusively by stars. Since IMCAT appears to have done a very good job at identifying the stars, we omitted the objects on the stellar locus at $I < 21$ in the colour-magnitude diagram in Fig. 4. The $R-I$ colours were evaluated using aperture magnitudes measured by IMCAT in a 1.5 arcsec aperture, corresponding to approximately twice the FWHM of the seeing disk.

We also examined the radial distribution of galaxies in the quasar fields as shown in Fig. 6. Here, we have taken the average of all fields, and counted galaxies in annuli of

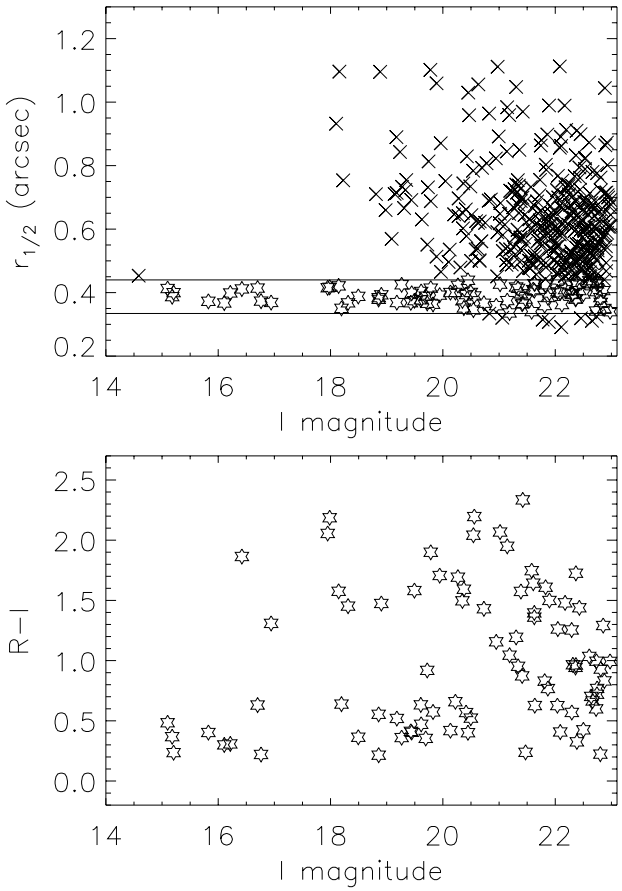

Figure 5. The upper plot shows the half-light radius of the objects in the four richest quasar fields as a function of magnitude. The stellar locus is clearly seen as the objects between the two horizontal lines (i.e. at seeing FWHM ≈ 0.8 arcsec). The lower plot shows a colour-magnitude diagram of the objects on the stellar locus.

100 kpc, and also corrected for missing areas due to large, extended foreground galaxies or stars. As seen from this figure, the distribution of galaxies seems to fall off outwards, but it is not completely clear whether the quasars lie at the centre of the distributions.

6 COMPARISON WITH OTHER STUDIES

In this section we compare our result with those obtained for other samples of RQQs. A compilation of results from the literature is shown in Fig. 7, where we have plotted mean clustering amplitudes as a function of median redshift and absolute quasar B magnitude.

The lowest redshift point in Fig. 7 is the mean amplitude found for 33 CfA Seyfert galaxies (both type 1 and 2) by DeRobertis et al. (1998), $B_{\rm gq} = 37.4 \pm 12.9$ Mpc$^{1.77}$. DeRobertis et al. compute mean clustering amplitudes separately for Seyfert 1 and Seyfert 2 galaxies, but these are consistent with each other in the case where the counting radius is 0.5 Mpc. Furthermore, Seyfert 2 galaxies are believed to contain hidden Seyfert 1 nuclei (e.g. Antonucci 1993), so we have chosen to use the mean for all Seyferts. Seyfert 1

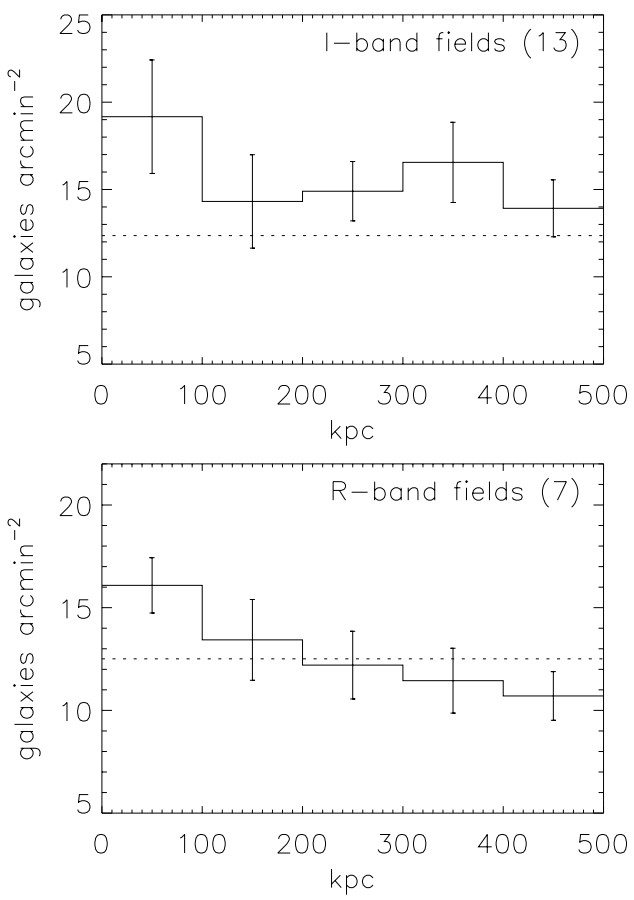

Figure 6. Average radial surface density profiles for the quasar fields. The quasars are located in the inner bins, and the error bars show the standard deviation in the mean. The dotted horizontal lines correspond to the average background count.

galaxies are the low-luminosity counterparts of RQQs, so we have assumed a mean nuclear luminosity of $M_B = -21$ for this sample. The median redshift is 0.0192 (from table 1, DeRobertis, Hayhoe & Yee (1998)).

Yee & Green (1987) found clustering amplitudes for BQS quasars in three redshift ranges, 0.00–0.15 (17 quasars), 0.15–0.30 (16) and 0.30–0.50 (7). They list the ratio of the mean amplitudes to the amplitude of the galaxy–galaxy correlation function, $B_{\rm gq}/B_{\rm gg}$. Assuming that $B_{\rm gg} = 67.5$ Mpc$^{1.77}$ (Davis & Peebles 1983), we find that $B_{\rm gq}$ is 113±36, 129±45 and 73±45 Mpc$^{1.77}$ in the three redshift ranges, respectively. To find the median absolute magnitude in the three sub-samples, we converted the apparent r magnitudes listed by Green & Yee (1984) and Yee et al. (1986) to R, and thereafter to B as described in Section 3. We found median absolute B magnitudes of −23.4, −24.24 and −25.83.

Smith et al. (1995) report a mean amplitude of $B_{\rm gq}/B_{\rm gg} = 1.0^{+0.7}_{-0.4}$ (2σ errors) for their sample of 169 $z \leq 0.3$ X-ray selected quasars with median redshift 0.15. The quasar M_V magnitudes in this sample span a wide range, from ≈ -27 to ≈ -20, but since there is no significant difference between the amplitudes of the angular correlation function for their high- and low luminosity subsamples, we have used the peak of the magnitude distribution, $M_V = -22.2$, converted to $M_B = -21.9$ assuming $B - V = 0.3$.

Fisher et al. (1996) find an average $B_{\rm gq}$ of 72±20 [h^{-1}Mpc]$^{1.77}$ for a sample of 14 optically bright RQQs, with a median redshift of 0.24, and a median M_V of −23.5 ($h = 1$). Assuming $B-V = 0.3$ and $h = 0.5$, we transformed to $B_{\rm gq} = 246 \pm 66$ Mpc$^{1.77}$ and $M_B = -24.71$. The RQQs in Fisher et al's sample are included in McLure & Dunlop's (2000) sample, along with seven other sources. McLure & Dunlop find a mean $B_{\rm gq}$ of 326±94 Mpc$^{1.77}$ and their sample has a median redshift of 0.165, and a median $M_V = -24.4$, which was converted to $M_B = -24.1$.

At median $z = 0.4$, we find the 32 RQQs in Ellingson et al's (1991a) sample. The mean amplitude is 16±45 Mpc$^{1.77}$, and we transformed the apparent quasar r magnitudes (given in table 2, Ellingson et al. (1991b)) to absolute B magnitudes as described in Section 3, and found a median $M_B = -22.78$.

The 82 X-ray selected quasars studied by Smith et al. (2000) cover the redshift range 0.3–0.7, and in their figure 8, $B_{\rm gq}$ is plotted as a function of $M_V - 5\log h$. By reading pairs of $B_{\rm gq}$ and $M_V - 5\log h$ off the axis of this figure, we estimate that the $z < 0.5$ and the $z > 0.5$ sub-samples have median $M_V - 5\log h \approx -21.8$ and ≈ -22.4, respectively. These were converted to $M_B = -23.00$ and -23.61 assuming $h = 0.5$ and $B - V = 0.3$. We found the mean amplitudes in these two redshift intervals to be approximately 6.13±2.95 and 4.52±7.88 [h^{-1}Mpc]$^{1.77}$. (We estimate that we can read off $M_V - 5\log h$ and $B_{\rm gq}$ with an accuracy of ±0.1 and ±5 [h^{-1}Mpc$^{1.77}$], respectively.) Smith et al. use a definition of $B_{\rm gq}$ which assumes that the clustering is stable in co-moving coordinates, whereas the definition by Longair & Seldner (1979) that we employ, assumes stable clustering in proper coordinates. We therefore transformed Smith et al's amplitudes to our convention by multiplying with $(1+z)^{3-\gamma}$, assuming that $\gamma = 1.77$, and that $z = 0.4$ and $z = 0.6$ for the two sub-samples. Thereafter, we transformed to the $h = 0.5$ case, and got mean amplitudes of 31.6±15.2 and 27.5±47.9 Mpc$^{1.77}$.

The next point along the redshift axis represents the results reported by Boyle, Shanks & Yee (1988) for eight BFSP quasars in the redshift range $0.55 < z < 0.7$, with mean $B_{\rm gq}/B_{\rm gg} = 2.3 \pm 1.3$. We have assumed $M_B = -23.5$ and a mean redshift of 0.625 for these quasars, since no other information is given.

Our own sample is plotted with a mean $B_{\rm gq} = 210 \pm 82$ (using Model 3), and a median redshift and M_B of 0.714 and −24.40.

Finally, the high-z point corresponds to the work by Boyle & Couch (1993), who find a mean $B_{\rm gq} = 3 \pm 40$ Mpc$^{1.77}$. The median M_B is −23.75, and we have assumed a mean redshift of 1.2.

There are several aspects about the quasar phenomenon, such as formation, fuelling and evolution, that we can learn about by looking at their environments as a function of redshift and AGN luminosity. But this has been difficult to do, both because there appears to be a wide range in richnesses within samples, and also because it requires good coverage of the redshift-luminosity plane. A figure like Fig. 7 might help, since looking at the mean $B_{\rm gq}$ values over a wide range in redshift and luminosity is more meaningful than relying on amplitudes found in single fields. The drawback is

of cause that Fig. 7 includes results from different studies with differing selection criteria, observations, analysis etc., and therefore contains uncontrollable selection effects and biasses. We are therefore careful with interpretations, and merely look at it as a useful way of comparing different surveys to see how they agree or disagree with each other as we move along the redshift and the luminosity axis.

Approximately half of the data points are significantly higher than the galaxy–galaxy clustering amplitude of $B_{\rm gg} = 67.5$ Mpc$^{1.77}$, whereas the other half is consistent with, or less than, $B_{\rm gg}$. The samples from the large cross-correlation studies (Smith et al. 1995; 2000; Boyle & Couch 1993) belong to the latter, along with Ellingson et al's sample, Yee & Green's high-z sample and the Seyfert sample of DeRobertis et al. The Seyfert sample is perhaps not so difficult to explain if we consider that spiral galaxies prefer field-like environments. If we further assume that low-luminosity quasars are mostly hosted by spiral galaxies, this might also explain Ellingson et al's result, but it does not explain why the mean amplitude of Yee & Green's bright, high-z sample is so low.

It is however noteworthy that the datapoints which agree with a galaxy environment richer than that of field galaxies are clustered around $M_B \approx -24$. The exceptions are Boyle & Couch's sample and Smith et al's (2000) $0.5 < z < 0.7$ sample, which have $B_{\rm gq} < B_{\rm gg}$. This may lead us to think that in these two studies, perhaps the galaxy excess (if present) was not detected. Their observations were done with filters that targets emission on the short-wavelength side of the 4000 Å break at the quasar redshift, and we found in Section 5 that the clustering signal in fields with a clear excess is weaker shortward of 4000 Å. Boyle & Couch used R and a wide VR passband (a combination of Johnson V and Kron-Cousins R), and at $z \approx 1.2$ both these filters target emission shortward of the 4000 Å break, and the sensitivity to early-type galaxies might not be particularly good. Also, the limiting magnitude, $R = 23$, might be somewhat too shallow in order to reach sufficiently faint into the luminosity function at these redshifts. Smith et al. (2000) used V-band, also corresponding to emission shortward of the 4000 Å break, at least at $z > 0.4$ where the bulk of their quasars are.

Most of the clustering studies similar to our (in terms of method and analysis) seem to agree fairly well that RQQ environments are different from field-like environments, both at high and at low redshifts. Yee & Green, Fisher et al. and McLure & Dunlop, looking at bright quasars at low redshifts, get clustering amplitudes consistent with ours, although Yee & Green's is a bit lower than the other two. Boyle et al's mean amplitude for BFSP quasars at $0.55 < z < 0.7$ also agree with ours at $z \approx 0.7$ and Fisher et al's at $z \approx 0.2$, so this raises the possibility that in fact there is little change in RQQ environments from $z \approx 0.2$ to $z \approx 0.7$–0.8. This is in agreement with recent studies that also find no changes in RLQ environments with redshift (Paper I; McLure & Dunlop 2000).

In light of the above, and considering the similarities in method and analysis, the low amplitude from Ellingson et al's work is difficult to explain. Since our quasar sample cover a wide range in B luminosity, there are several quasars at similar luminosities to Ellingson et al's quasars. The six quasars at $M_B > -23.5$ in our sample have a mean $B_{\rm gq} = 237 \pm 78$ (Model 3), which is very different from Ellingson et al's 16±45 Mpc$^{1.77}$. The remaining 14 quasars at $M_B < -23.5$ have a mean amplitude of 196±110 Mpc$^{1.77}$ (Model 3), so we find no difference between high- and low-luminosity sub-samples. Since the six quasars at $M_B > -23.5$ have a median redshift of 0.720, i.e. higher than Ellingson et al's $z = 0.4$, it might seem as though the environmental richness change with redshift for the lower luminosity quasars, but not for the high luminosity ones. This is perhaps somewhat odd since we have no reason to believe that our amplitudes have a systematic error relative to Ellingson et al's.

In Paper I, we found that the $B_{\rm gq}$'s for our RLQ fields lay in the same range as those found for RLQs by Ellingson et al., and the mean amplitudes were consistent with each other. Furthermore, for the RLQ MRC 0405−123, Yee & Ellingson (1993) found $B_{\rm gq} = 905 \pm 277$, whereas we found 579±179 Mpc$^{1.77}$, i.e. slightly lower, but still in agreement with each other. So it seems unlikely that our amplitudes are systematically different from Ellingson et al's. One possible explanation for the discrepancy may be the inhomogeneity of Ellingson et al's sample. Their sample was chosen from the Hewitt-Burbidge catalogue (Hewitt & Burbidge 1987), which is an incomplete compilation of quasars, but nevertheless the best catalogue available at that time. There could be some subtle bias in this sample that causes the highest $B_{\rm gq}$ fields to be excluded. E.g. if we clip out the five highest $B_{\rm gq}$'s in our sample, we get a similar result as Ellingson et al., most RQQs having $B_{\rm gq}$ less than 300 Mpc$^{1.77}$ and a mean consistent with their.

We have seen that, whereas some surveys find that RQQs live in field-like environments, others agree with our survey finding a richer than average galaxy density around RQQs. But the question whether the disagreement is due to selection effects caused by redshift and/or luminosity, appears difficult to answer.

7 A DIRECT COMPARISON WITH RLQ ENVIRONMENTS

In Paper I, we investigated the galaxy environments around 21 steep-spectrum RLQs. The current sample of RQQs matches the RLQ sample in redshift and B magnitude, and both samples were observed with the same telescope and analysed in the same manner. This offer us a direct and internally consistent way of comparing the galaxy environments around RLQs and RQQs at the same epoch and with similar AGN luminosities.

In Fig. 8, we show $B_{\rm gq}$ as function of z and M_B for both samples (using Model 3 for the background counts), where it can be seen that they span the same wide range in environmental richness. The mean clustering amplitude for the RLQs is 213±66 (Model 3), and redoing the RLQ fields using Model 1 and 2 for the background counts, the mean $B_{\rm gq}$'s become 214±83 and 224±55 Mpc$^{1.77}$, respectively. We thus find that the mean clustering amplitudes for the RLQ and the RQQ samples are practically indistinguishable, i.e. *on average, there is no difference in the galaxy environments on 0.5 Mpc scales for the RQQs and the RLQs.*

The mean and the median $B_{\rm gq}$'s for the two quasar samples are summarized in Table 7. The median $B_{\rm gq}$'s are

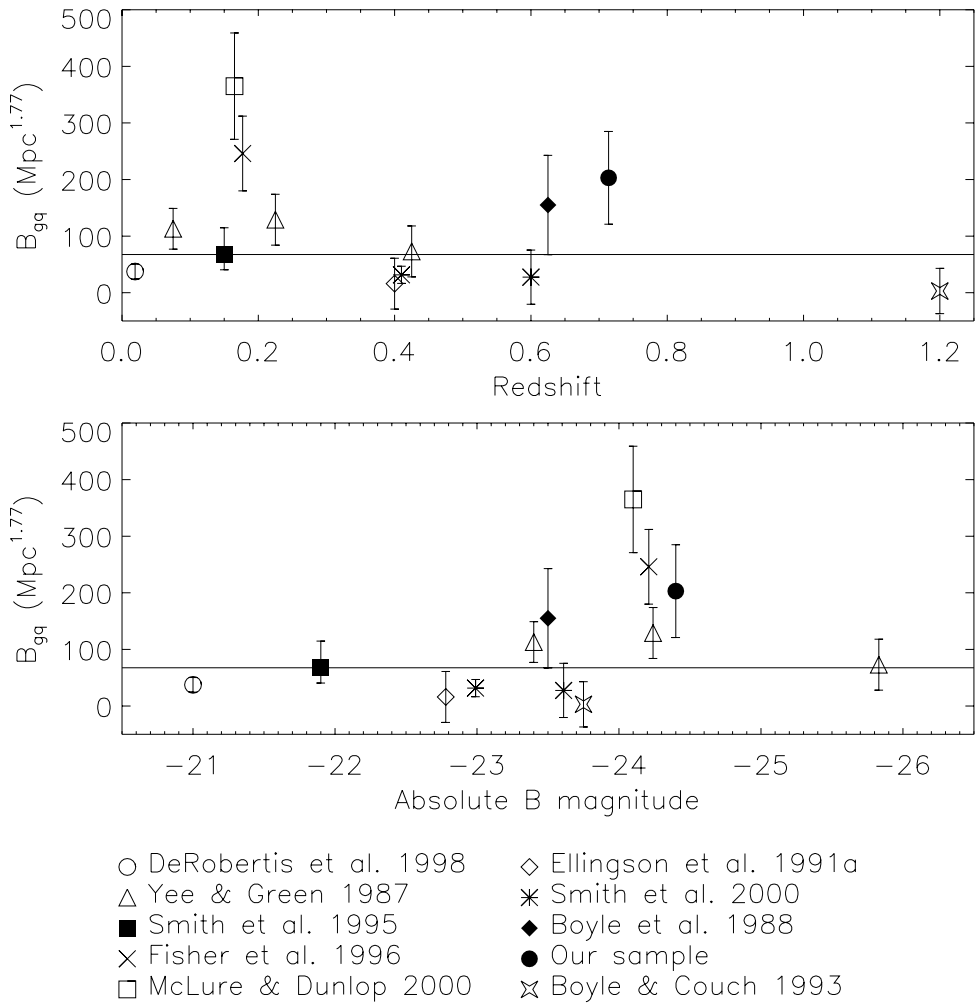

Figure 7. RQQ environment as a function of redshift and M_B. The horizontal line indicates the amplitude of the local galaxy–galaxy correlation function, $B_{\rm gg} = 67.5$ Mpc$^{1.77}$ (Davis & Peebles 1983).

seen to be generally lower than the mean values, but this is not very significant. The intrinsic scatter seems to be smaller for the RLQs, and is more comparable to $\Delta B_{\rm gq}$ than for the RQQs. A KS test gives a significance level of 0.72 for the null hypothesis that the two samples are drawn from the same distribution, i.e. the two samples are consistent with being drawn from the same distribution.

This result is contrary to the traditional picture that the environments of RLQs and RQQs differ, i.e. that RQQs are found in systematically poorer environments than RLQs. It was reported in the similar study by Ellingson et al. (1991a) that RLQs inhabited poorer environments than RQQs at $z \sim 0.4$–0.5. However, at $z \approx 0.2$, Fisher et al. (1996) and McLure & Dunlop (2000) compare samples of RLQs and RQQs matched in redshift and luminosity, and find no significant differences, hence our result at $0.5 \leq z \leq 0.8$ is consistent with these findings at low redshifts. Also at higher redshifts, $z \approx 1.1$, Hutchings et al. (1995) find evidence for similar environments around RLQs and RQQs, compact groups or clusters of star-forming galaxies. It thus appears that both RLQs and RQQs at low to intermediate redshifts on average occupy the same type of environment, consistent with poorer galaxy clusters, and that the environments of, at least powerful, RLQs and RQQs do not change with redshift, possibly not even out to $z \sim 1$.

Our result is also consistent with the findings that at low redshifts powerful RLQs and RQQs appear to be hosted by luminous galaxies with luminosities above the break in the luminosity function (e.g. Dunlop et al. 1993; McLeod & Rieke 1994; Taylor et al. 1996; Bahcall et al. 1997; Boyce et al. 1998). Luminous early-type galaxies are known to prefer rich environments, and it thus follows that powerful quasars hosted by these galaxies also appear in rich environments. There are some evidence that the hosts of powerful RQQs are massive ellipticals, but the results are still somewhat inconclusive. Bahcall et al. (1997) find more RQQs in elliptical hosts than in spiral hosts, but note that the quasars also appear in interacting systems and spiral galaxies. McLure et al. (1999) find that all $M_R < -24$ RQQs in their sample are hosted by massive ellipticals and Hughes et al. (2000) present off-nuclear spectra of luminous AGN, and identify the 4000 Å break in the stellar component of the host in many cases.

For completeness, we mention that if we exclude the

Table 6. Mean and median clustering amplitudes for 21 RLQs and 20 RQQs. Model 1–3 correspond to different ways of correcting for background galaxies. The intrinsic scatter in the $B_{\rm gq}$ distribution is denoted $\sigma_{\rm int}$ and was calculated as $(\sigma^2_{B_{\rm gq}} + \Delta B^2_{\rm gq})^{1/2}$, where $\sigma_{B_{\rm gq}}$ is the standard deviation of the $B_{\rm gq}$ distribution and $\Delta B_{\rm gq}$ is the measurement error.

	Model 1			Model 2			Model 3		
Sample	Mean	Median	$\sigma_{\rm int}$	Mean	Median	$\sigma_{\rm int}$	Mean	Median	$\sigma_{\rm int}$
RQQ	336±77	229	387±54	212±74	151	276±72	210±82	131	315±73
RLQ	214±83	264	332±75	224±55	165	172±86	213±66	178	236±76

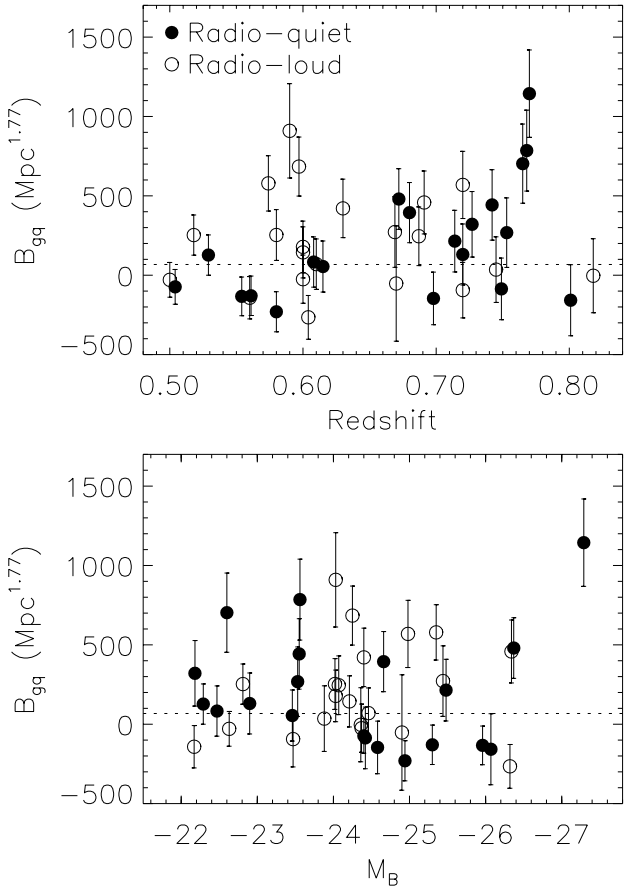

Figure 8. $B_{\rm gq}$ as a function of redshift and quasar absolute magnitude for RLQs and RQQs. The dotted lines refer to the value of the amplitude of the local galaxy–galaxy correlation function, $B_{\rm gg} = 67.5$ Mpc$^{1.77}$ (Davis & Peebles 1983).

three quasars with radio powers $> 1.3 \times 10^{25}$ W Hz^{-1} (the two BQS quasars and LBQS 2348+0210), the mean becomes 191±73 Mpc$^{1.77}$ (Model 3), so there is little change, and the mean is still consistent with the mean $B_{\rm gq}$ for the RLQs. This is also the case when we exclude the two BQS quasars on the basis that the BQS suffers from incompleteness, the mean being 177±71 Mpc$^{1.77}$. The mean amplitude for the sample when the seven radio-detected quasars are excluded is 178±82 Mpc$^{1.77}$.

8 DISCUSSION

In Paper I, we found that the clustering amplitudes in RLQ fields seemed to correlate with radio luminosity instead of redshift. Extrapolating this to the RQQs with radio luminosities two–three orders of magnitude lower, one might expect them to be sited in poorer environments than the RLQs. Instead we find that, on average, the environments around RLQs and RQQs are indistinguishable. This suggests that the process that determines the radio loudness is not dependent on the environment on Mpc scales, but may instead be found in the central regions of the host galaxy. This is consistent with the correlation found by Rawlings & Saunders (1991) between narrow-line luminosity and radio luminosity in radio galaxies, and the radio-optical correlation in steep-spectrum RLQs found by Serjeant et al. (1998). These correlations link the production of optical emission lines in the nuclear regions to the production of large-scale radio emission, implying that the fuelling of radio jets is linked to accretion onto the black hole.

If, e.g. as a result of galaxy interactions and mergers, a RLQ is born, the environment into which the source expands may affect its radio luminosity, e.g. enhancing it (Barthel & Arnaud 1996), and we observe a weak correlation between $B_{\rm gq}$ and radio luminosity (Paper I), but the presence of the radio loudness itself would be independent of environment. If a RQQ is born, we would perhaps expect a correlation between quasar optical luminosity and $B_{\rm gq}$ (also for RLQs), but this would be harder to detect, both because the nuclear optical luminosities probe much smaller regions than the radio luminosity does, and because the optical luminosity may vary.

We expect a relation between environmental richness and quasar optical luminosity since the luminosity created by accretion onto the black hole scales with the black hole mass. According to the Kormendy & Richstone (1995) and the Magorrian et al. (1998) relations, the mass of a black hole scales with the luminosity (or the mass) of the spheroidal component of the host galaxy. (See also Ferrarese & Merritt (2000) who find a tight relation between black hole mass and velocity dispersions of bulges.) Early-type galaxies, being bulge-dominated, and likely to reside in rich environments, are therefore expected to host the most massive black holes, and thus the most luminous quasars. McLure & Dunlop (2000) looked at $B_{\rm gq}$ vs nuclear luminosity as found from the Magorrian et al. relation, but found that the correlation was not statistically significant.

Being sited in equally rich environments, RLQs and RQQs are equally replenished by fuel from their surroundings, so both quasar populations would survive for similar amounts of time. This implies that the fraction of radio-loud

quasars would be independent of redshift, and agrees well with Goldschmidt et al. (1999) who find that the radio-loud fraction depends on optical luminosity, not redshift.

There does not appear to be evidence for an epoch dependence in $B_{\rm gq}$ between $z \approx 0.2$ and ≈ 0.8. It is however not unthinkable that there could be one for RQQs, but at higher redshifts, $z \sim 1$–2. This is because hosts of powerful RQQs change with redshift; at low-z, they are giant elliptical galaxies with $L > L^*$ (the less powerful ones have spiral hosts), whereas at high redshifts they are $\sim L^*$ galaxies (e.g. Hutchings 1995b; Ridgway et al. 2000; Kukula et al. 2000). Radio galaxies do not change over the whole interval $z \sim 2$ to 0 (Lacy, Bunker & Ridgway 2000), so according to radio-loud unified schemes, RLQ hosts should behave in the same manner. Aragón-Salamanca, Ellis & O'Brien (1996) do in fact find a significant excess around RLQs at $z \approx 2.5$ that is not seen around RQQs at the same redshift (four RLQs and six RQQs).

The change in the hosts of RQQs with redshift is probably related to the huge increase in their space density between $z \sim 0-1$ and $z \sim 2-3$. In a model for the formation and evolution of quasars, Kauffmann & Haehnelt (2000) link their evolution to the hierarchical build-up of galaxies, and predict that quasars at a given luminosity should be found in progressively less luminous host galaxies towards higher redshifts. But this explanation cannot work for the radio-louds. The fact that the hosts of the radio-louds do not appear to evolve strongly may be because there is a strong link between the mass of the black hole and the ability to produce powerful jets (Lacy, Ridgway & Trentham 2000; Laor 2000). Thus only objects whose black holes (and therefore hosts) are already massive at high redshifts can be radio loud.

In principle, we can also quote a lower limit to the comoving space density of Abell 1–2 clusters at $z \sim 0.7$. The space density of quasars at $z = 0.7$ is $\sim 3 \times 10^{-6}$ Mpc^{-3}‡ (Boyle et al. 2000), and since ≈ 10 per cent of the quasars in our sample live in Abell 1–2 clusters, this would correspond to $>3{\times}10^{-7}$ Abell 1–2 clusters per Mpc^3 at $z \sim 0.7$. This is potentially interesting for cosmology and may even constrain Ω_0, because predictions of cluster number densities at high redshifts are highly model dependent (Lilje 1992).

It is also interesting to note that this can be used to set a lower limit to the duty cycle of quasars. Normally, only upper limits are given based on e.g. central black hole masses in Seyferts. The duty cycle of quasars can be thought of as the probability for a black hole to accrete, or the ratio of active to dormant + active quasars at a certain epoch. We know from our study that the fraction of active quasars living in Abell 1–2 clusters at $z \approx 0.7$ is ≈ 0.10, and we also know that the number of clusters hosting a black hole (both dormant and active) must be less than the number of Abell 1–2 clusters at the present epoch. If we assume that the typical X-ray luminosity of such clusters is 10^{43} erg s^{-1}, the local cluster density is $\approx 2{\times}10^{-5}$ (Rosati et al. 1998), and thus the lower limit to the quasar duty cycle is $\approx 0.1{\times}3{\times}10^{-6}/2{\times}10^{-5}$, i.e. about 1 per cent. This only applies to RQQs living in Abell 1–2 clusters, and the present-day duty cycle of such systems is probably very low. The continous accretion phase cannot last very long, and at some point it stops, perhaps when the cluster virializes.

‡ Found by integrating Boyle et al's (2000) quasar luminosity function between the absolute magnitude limits of our survey. We used the expression $\frac{\Phi(M_B,z)}{\Phi(M_B^*)} = [10^{-0.4[(\alpha-1)(M_B-M_B^*(z))]} + 10^{-0.4[(\beta-1)(M_B-M_B^*(z))]}]^{-1}$, which is different from that given in the paper, since we suspect that a misprint may have occurred.

9 CONCLUSIONS

The RQQs studied in this paper live in a diversity of environments, from field-like environments to galaxy clusters as rich as Abell class 1–2. On average, the sample has a clustering amplitude corresponding to groups or poorer clusters of Abell class ≈ 0, and is *indistinguisable* from the mean amplitude found for a sample of RLQs matched in redshift and AGN luminosity.

Our finding that the average environment around RLQs and RQQs at $0.5 \leq z \leq 0.8$ is statistically indistinguishable agrees with what is found for powerful quasars at $z \approx 0.2$ by Fisher et al. (1996) and McLure & Dunlop (2000). There is agreement also in terms of the amount of clustering, suggesting that quasar environments, for both RLQs and RQQs, do not undergo much evolution between $z \approx 0.2$ and ≈ 0.8. These results are consistent with host galaxy studies finding that both powerful RLQs and RQQs live in massive, elliptical galaxies (e.g. Dunlop et al. 1993; Bahcall et al. 1997; McLure et al. 1999). We therefore believe that the consensus that RQQs occupy systematically poorer environments than RLQs should be put under doubt.

Since our RQQs on average appear in cluster environments they are most likely biased with respect to galaxies. Galaxy clusters are also biased (e.g. Lilje & Efstathiou 1988; Croft, Dalton & Efstathiou 1999), so the RQQs in clusters must have a bias factor that is greater than that for normal galaxies. This suggests that RQQs can not be used as unbiased tracers of galaxies when studying large scale stucture using quasars surveys.

That RLQs and RQQs on average live in equally rich environments implies that the origin of the radio loudness is not linked to the environments on Mpc scales, but may instead be buried within the central parts of the host galaxy. This is consistent with the suggestion that the fuelling of radio jets is linked to accretion onto a central black hole (Rawlins & Saunders 1991; Serjeant et al. 1998).

A colour-magnitude diagram of the richest RQQ fields in this study shows hints of a red sequence at the expected colour of $z = 0.7$–0.8 early-type galaxies. With spectroscopy, these fields will likely turn out to contain galaxy clusters at $z = 0.7$–0.8. RLQs and radio galaxies are often used to find and study galaxy clusters at higher redshifts, and our result that RLQs and RQQs inhabit similar environment at $z \sim 0.7$–0.8 should therefore increase the pool of likely cluster candidates at high redshifts. This may be important for theories of galaxy formation, since it allows us to find and study high redshift galaxy clusters that are not selected on the basis of extreme optical or X-ray luminosity.

Acknowledgements

We are grateful to the staff at the NOT for help during the observations, to D. Burstein for providing maps of galactic extinction in electronic form, and to N. Kaiser for the IMCAT software. MW wishes to thank H. Dahle for valuable help with IMCAT, L. Borgonovo for discussions, and also D. Koo, C. Willmer and P. Guhathakurta for discussions during a visit to UCSC. PBL and MW acknowledges travel support from the Norwegian Research Council, and MW also acknowledges the STINT Exchange Program Stockholm Observatory-Astronomy/UC Santa Cruz. ML acknowledges support from NSF grants AST-98-02791 and AST-98-02732, and conducted his work under the auspices of the U.S. Department of Energy at the University of California Lawrence Livermore National Laboratory under contract No. W-7405-Eng-48.

This research is based on observations made with the Nordic Optical Telescope which is is operated on the island of La Palma jointly by Denmark, Finland, Iceland, Norway and Sweden, in the Spanish Observatorio del Roque de los Muchachos of the Instituto de Astrofisica de Canarias. The data presented here have in part been taken using ALFOSC, which is owned by the Instituto de Astrofisica de Andalucia (IAA) and operated at the Nordic Optical Telescope under agreement between IAA and NBIfAFG of the University of Copenhagen.

IRAF is distributed by the National Optical Astronomy Observatories, which are operated by the Association of Universities for Research in Astronomy, Inc., under cooperative agreement with the National Science Foundation. This research has made use of the NASA/IPAC extragalactic database (NED) which is operated by the Jet Propulsion Laboratory, California Institute of Technology, under contract with the National Aeronautics and Space Administration.

REFERENCES

Antonucci R., 1993, ARA&A, 31, 473
Aragón-Salamanca A., Ellis R.S., O'Brien K.S., 1996, MNRAS, 281, 945
Arimoto A., Yoshii Y., 1987, A&A, 173, 23
Bahcall J.N., Soneira R.M., 1981, ApJS, 47, 357
Bahcall J.N., Kirhakos S., Saxe D.H., Schneider D.P., 1997, ApJ, 479, 642
Barthel P.D., Arnaud K.A., 1996, MNRAS, 238, L45
Becker R.H., White R.L., Helfand D.J., 1995, ApJ, 450, 559
Best P., 2000, MNRAS, 317, 720
Blundell K.M., Beasley A.J., 1998, MNRAS, 299, 165
Blundell K.M., Beasley A.J., Lacy M., Garrington S.T., 1996, ApJ, 468, L91
Boyce P.J. et al., 1998, MNRAS, 298, 121
Boyle B.J., Couch W.J., 1993, MNRAS, 264, 604
Boyle B.J., Fong R., Shanks T., Peterson B.A., 1990, MNRAS, 243, 1
Boyle B.J., Shanks T., Croom S.M., Smith R.J., Miller L., Loaring N., Heymans C., 2000, MNRAS, 317, 1014
Boyle B.J., Shanks T., Yee H., 1988, in IAU Symp. 130, Large Scale Structues of the Universe, ed. Audouze J., Pelletan M.C. & Szalay A., Dordrecht, Kluwer, 576
Burstein D., Heiles C., 1982, AJ, 87, 1165
Cardelli J.A., Clayton G.C., Mathis J.S., 1989, ApJ, 345, 245
Chapman S.C., McCarthy P., Persson S.E., 2000, AJ, 120, 1612
Christian C.A., Adams M., Barnes J.V., Butcher H., Hayes D.S., Mould J.R., Siegel M., 1985, PASP, 97, 363
Clowe D., Luppino G.A., Kaiser N., Henry J.P., Gioia I.M., 1998, ApJ, 497, L61
Condon J.J., Cotton W.D., Greisen E.W., Yin Q.F., Perley R.A., Taylor G.B., Broderick J.J., 1998, AJ, 115, 1693
Croft R.A.C., Dalton G.B., Efstathiou G., 1999, MNRAS, 305, 547
Croom S.M., Shanks T., 1999, MNRAS, 303, 411
Davis M., Peebles P.J.E., 1983, ApJ, 267, 465
Deltorn J.-M., LeFèvre O., Crampton D., Dickinson M., 1997, ApJ, 483, L21
DeRobertis M.M., Hayhoe K., Yee H.K.C., 1998, ApJS, 115, 163
DeRobertis M.M., Yee H.K.C., Hayhoe K., 1998, ApJ, 496, 93
Dickinson M., 1994, in Hippelein H. et al., eds, Galaxies in the Young Universe. Springer-Verlag, Berlin, p. 144
Dunlop J.S., Taylor G.L., Hughes D.H., Robson E.I., 1993, MNRAS, 264, 455
Ellingson E., Yee H.K.C., Green R.F., 1991a, ApJ, 371, 49
Ellingson E., Yee H.K.C., Green R.F., 1991b, ApJS, 76, 455
Falcke H., Sherwood W., Patnaik A.R., 1996, ApJ, 471, 106
Fan X., et al., 1999, AJ, 118, 1
Ferrarese L., Merritt D., 2000, ApJ, 539, L9
Ferreras I., Silk J., 2000, ApJ, 532, 193
Fisher K.B., Bahcall J.N., Kirhakos S., Schneider D.P., 1996, ApJ, 468, 469
Fukugita M., Shimasaku K., Ichikawa T., 1995, PASP, 107, 945
Gladders M.D., López-Cruz O., Yee H.K.C., Kodama T., 1998, ApJ, 501, 571
Goldschmidt P., Kukula M.J., Miller L., Dunlop J.S., 1999, ApJ, 511, 612
Goldschmidt P., Miller L., La Franca F., Cristiani S., 1992, MNRAS, 256, 65P
Green R.F., Yee H.K.C., 1984, ApJS, 54, 495
Guiderdoni B., Rocca-Volmerange B., 1988, A&AS, 74, 175
Guzzo L., Strauss M.A., Fisher K.B., Giovanelli R., Haynes M.P., 1997, ApJ, 489, 37
Hall P.B., Green R.F., 1998, ApJ, 507, 558
Hewett P.C., Foltz C.B., Chaffee F.H., 1995, AJ, 109, 1498
Hewitt A., Burbidge G., 1987, ApJS, 63, 1
Hintzen P., Romanishin W., Valdes F., 1991, ApJ, 366, 7
Hooper E.J., Impey C.D., Foltz C.B., Hewett P.C., 1996, ApJ, 473, 764
Hughes D.H., Kukula M.J., Dunlop J.S., Boroson T., 2000, MNRAS, 316, 204
Hutchings J.B., 1995a, AJ, 109, 928
Hutchings J.B., 1995b, AJ, 110, 994
Hutchings J.B., Crampton D., Johnson A., 1995, AJ, 109, 73
Hutchings J.B., Crampton D., Morris S.L., Durand D., Steinbring E., 1999, AJ, 117, 1109
Kaiser N., Squires G., Broadhurst T., 1995, ApJ, 449, 460
Kauffmann G., Charlot S., 1998, MNRAS, 294, 705
Kauffmann G., Haehnelt M., 2000, MNRAS, 311, 576
Kellerman K.I., Sramek R., Schmidt M., Shaffer D.B., Green R., 1989, AJ, 98, 1195
Kent S.M., 1985, PASP, 97, 165
Kormendy J., Richstone D., 1995, ARA&A, 33, 581
Kukula M.J., Dunlop J.S., McLure R.J., Miller L., Percival W.J., Baum S.A., O'Dea C.P., 2000, MNRAS, submitted (astro-ph/0010007)
Lacy M., Bunker A.J., Ridgway S., 2000, AJ, 120, 68
Lacy M., Ridgway S., Trentham N., 2000, in Biretta et al., eds., Lifecycles of Radio Galaxies, New Astronomy Reviews, in press (astro-ph/9909163)
LaFranca F., Gregorini L., Cristiani S., de Ruiter H., Owen F., 1994, AJ, 108, 1548
Landolt A.U., 1992, AJ, 104, 340
Laor A., 2000, ApJL, 543, 111

Larson R.B., 1975, MNRAS, 173, 671
Lilje P.B., 1992, ApJL, 386, 33
Lilje P.B., Efstathiou G., 1988, MNRAS, 231, 635
Lilly S.J., Tresse L., Hammer F., Crampton D., LeFèvre O., 1995, ApJ, 455, 108
Longair M.S., 1981, in High Energy Astrophysics, Cambridge Univ. Press, p. 171
Longair M.S., Seldner M., 1979, MNRAS, 189, 433
Loveday J., Maddox S.J., Efstathiou G., Peterson B.A., 1995, ApJ, 442, 457
Lubin L.M., Brunner R., Metzger M.R., Postman M., Oke J.B., 2000, ApJ, 531, L5
Luppino G.A., Kaiser N., 1997, ApJ, 475, 20
Magorrian J. et al., 1998, ApJ, 115, 2285
McLeod K.K., Rieke G.H., 1994, ApJ, 431, 137
McLure R.J., Dunlop J.S., 2000, MNRAS, submitted (astro-ph/0007219)
McLure R.J., Kukula M.J., Dunlop J.S., Baum S.A., O'Dea C.P., Hughes D.H., 1999, MNRAS, 308, 377
Metcalfe N., Shanks T., Fong R., Jones L.R., 1991, MNRAS, 249, 498
Miller P., Rawlings S., Saunders R., 1993, MNRAS, 263, 425
Oke J.B., 1972, ApJS, 27, 21
Percival W.J., Miller L., McLure R.J., Dunlop J.S., 2000, MNRAS,
Rawlings S., Saunders R., 1991, Nat., 349, 138
Riley J.M., Rawlings S., McMahon R.G., Blundell K.M., Miller P., Lacy M., Waldram E.M., 1999, MNRAS, 307, 293
Ridgway S., Heckman T., Calzetti D., Lehnert M., 2000, in Biretta et al., eds., Lifecycles of Radio Galaxies, New Astronomy Reviews, in press (astro-ph/9911049)
Rosati P., Della Ceca R., Norman C., Giacconi R., 1998, ApJL, 492, 21
Schmidt M., Green R.F., 1983, ApJ, 269, 352
Serjeant S.B.B., 1996, DPhil Thesis, Univ. Oxford
Serjeant S., Rawlings S., Maddox S.J., Baker J.C., Clements D., Lacy M., Lilje P.B., 1998, MNRAS, 294, 494
Shanks T., Boyle B.J., Croom S.M., Loaring N., Miller L., Smith R.J., 2000, in Mazure A., LeFèvre O., LeBrun V., eds., Clustering at high redshift, ASP Conf. Ser. 200, 57
Smail I., Hogg D.W., Yan L., Cohen J.G., 1995, ApJ, 449, L105
Smith E.P., Heckman T.M., 1990, ApJ, 348, 38
Smith R.J., Boyle B.J., Maddox S.J., 1995, MNRAS, 277, 270
Smith R.J., Boyle B.J., Maddox S.J., 2000, MNRAS, 313, 252
Smith E.P, O'Dea C.P., Baum S.A, 1995, ApJ, 441, 113
Sramek R.A., Weedman D.W., 1980, ApJ, 238, 435
Tanaka I., Yamada T., Aragón-Salamanca A., Kodama T., Miyaji T., Ohta K., Arimoto N., 2000, ApJ, 528, 123
Taylor G.L., Dunlop J.S., Hughes D.H., Robson E.I., 1996, MNRAS, 283, 930
Teplitz H.I., McLean I.S., Malkan M.A., 1999, ApJ, 520, 469
Toomre A., Toomre J., 1972, ApJ, 178, 623
Valdes F., 1989, in Grosbøl P.J., Murtagh F., Warmels R.H., eds, Proceedings of the 1st ESO/ST-ECF Data analysis workshop. ESO, Garching bei Múnchen, p.35
White R.L. et al., 2000, ApJS, 126, 133
Wold M., Lacy M., Lilje P.B., Serjeant S., 2000, MNRAS, 316, 267 (Paper I)
Wurtz R., Stocke J.T., Ellingson E., Yee H.K.C., 1997, ApJ, 480, 547
Yates M.G., Miller L., Peacock J.A., 1989, MNRAS, 240, 129
Yee H.K.C., Ellingson E., 1993, ApJ, 411, 43
Yee H.K.C., Green R.F., 1984, ApJ, 280, 79
Yee H.K.C., Green R.F., 1987, ApJ, 319, 28
Yee H.K.C., López-Cruz O., 1999, AJ, 117, 1985
Yee H.K.C., Green R.F., Stockman H.S., 1986, ApJS, 62, 681

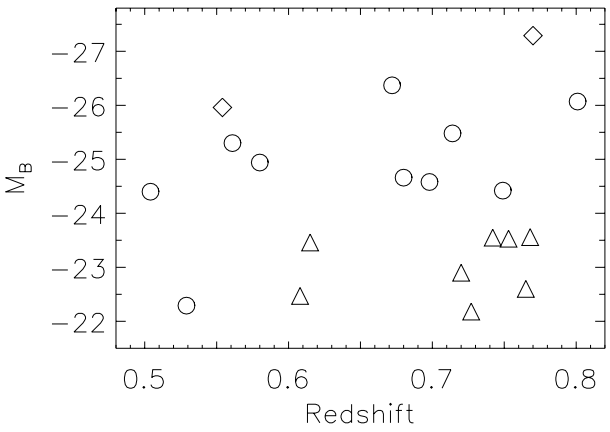
−27
−26
−25
−24
−23
−22
M_B
0.5
0.6
0.7
0.8
Redshift

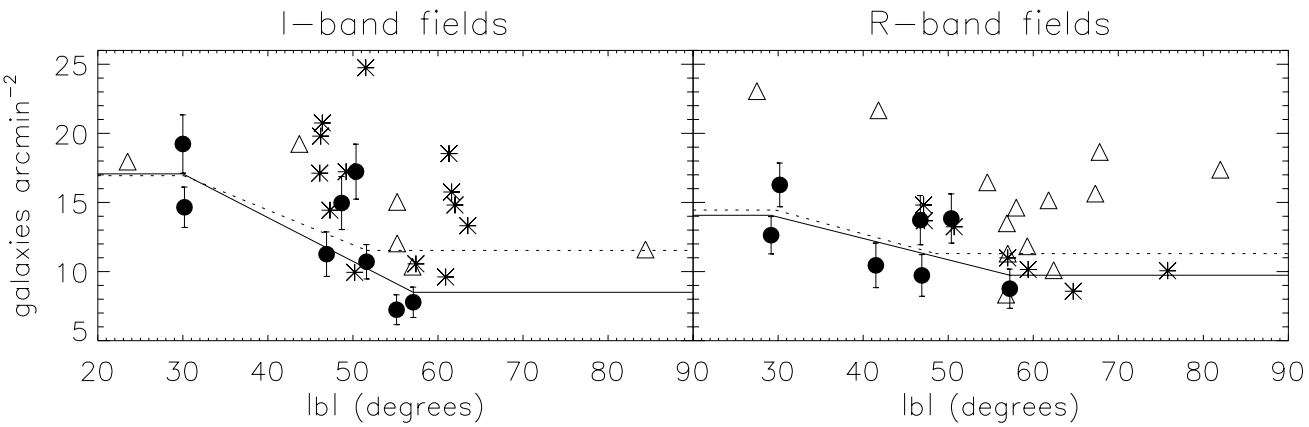
I−band fields
R−band fields
galaxies arcmin^{-2}
25
20
15
10
5
20
30
40
50
60
70
80
90
|b| (degrees)

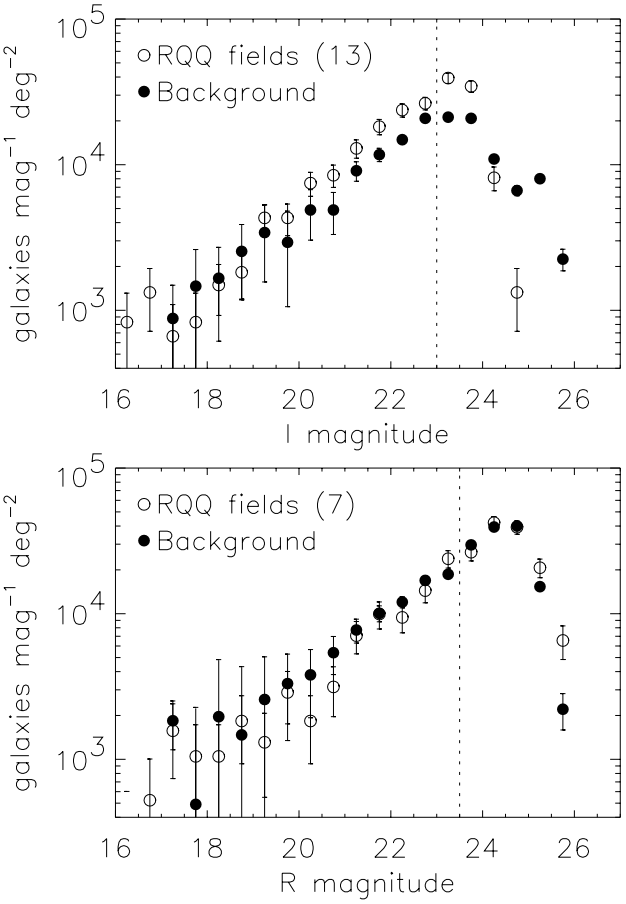
RQQ fields (13)
Background
galaxies mag^{-1} deg^{-2}
I magnitude
RQQ fields (7)
Background
galaxies mag^{-1} deg^{-2}
R magnitude

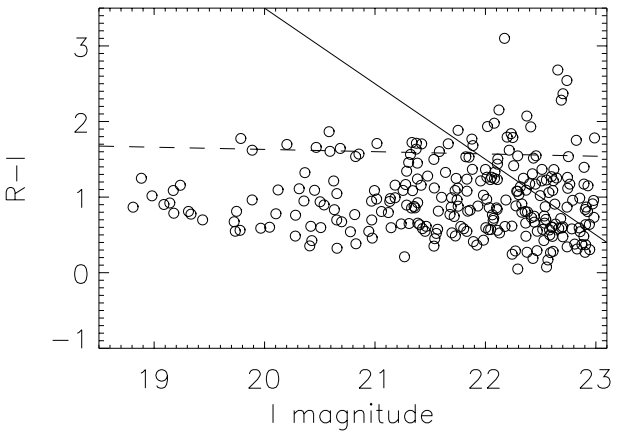
R−I
3
2
1
0
−1
19
20
21
22
23
I magnitude

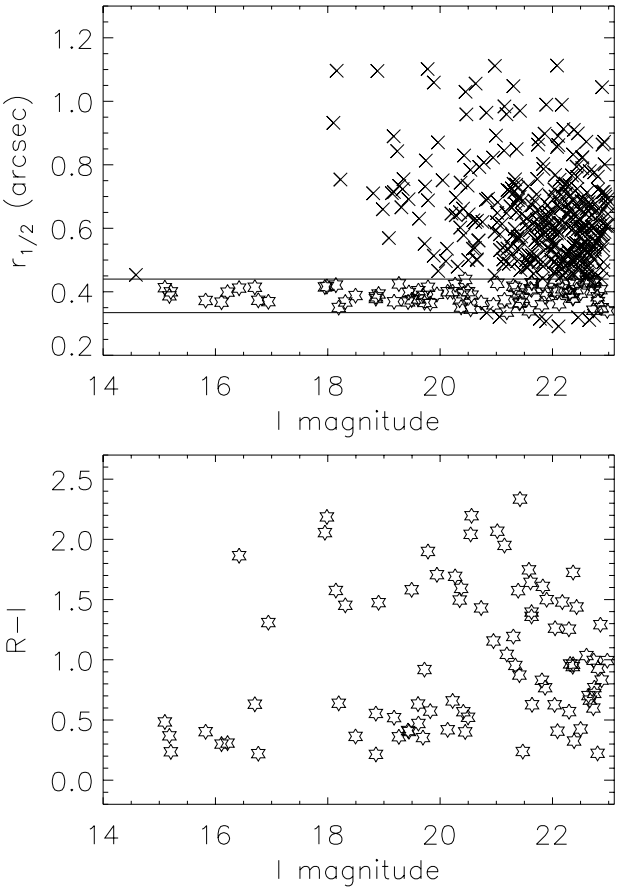
1.2
1.0
0.8
0.6
0.4
0.2
$r_{1/2}$ (arcsec)
14
16
18
20
22
I magnitude
2.5
2.0
1.5
1.0
0.5
0.0
R−I
14
16
18
20
22
I magnitude

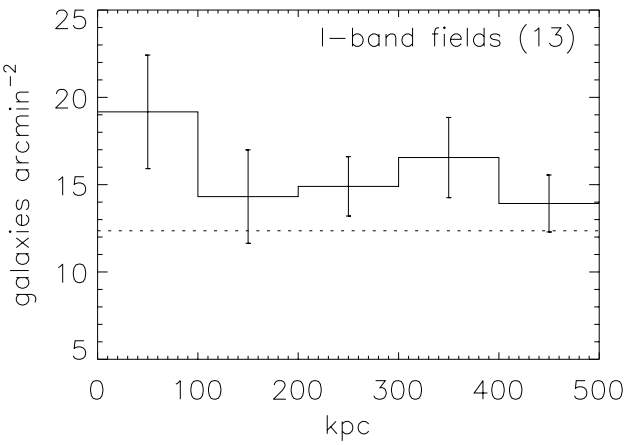
I−band fields (13)
galaxies arcmin^{-2}
25
20
15
10
5
0
100
200
300
400
500
kpc

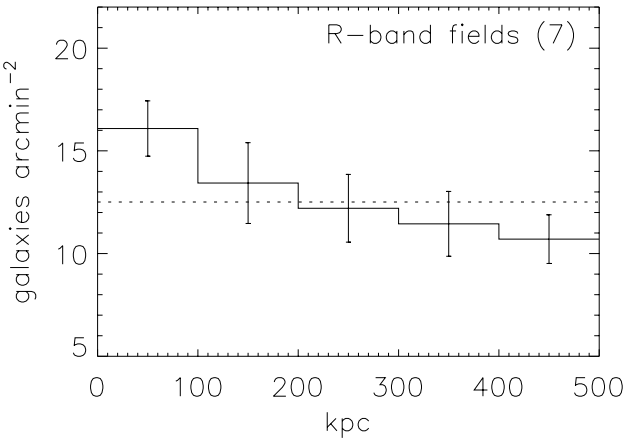
R−band fields (7)
galaxies arcmin^{-2}
20
15
10
5
0
100
200
300
400
500
kpc

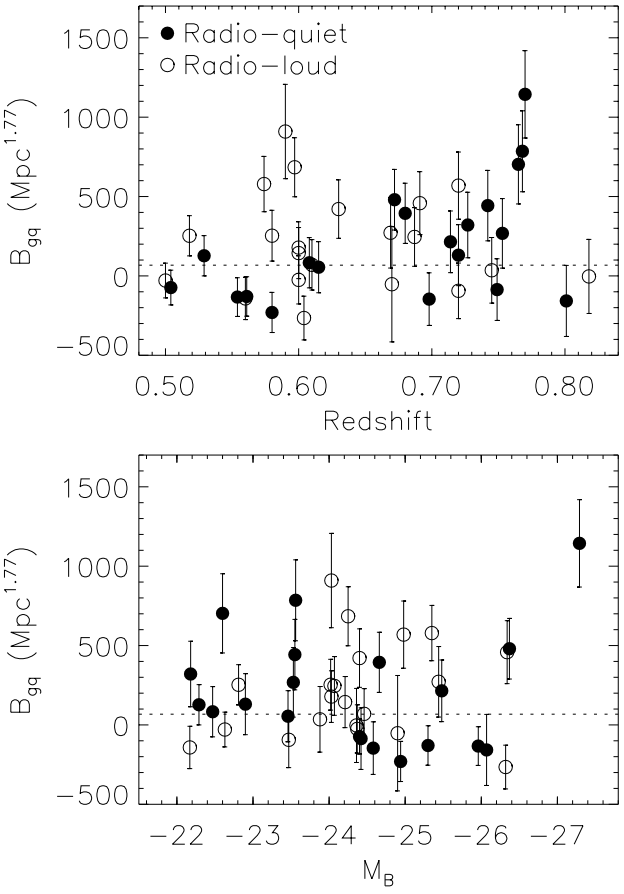
Radio−quiet
Radio−loud
1500
1000
500
0
−500
B_{gq} (Mpc$^{1.77}$)
0.50
0.60
0.70
0.80
Redshift
−22
−23
−24
−25
−26
−27
M_B